GEAR TECHNOLOGY

The Journal of Gear Manufacturing

JANUARY/FEBRUARY 1988

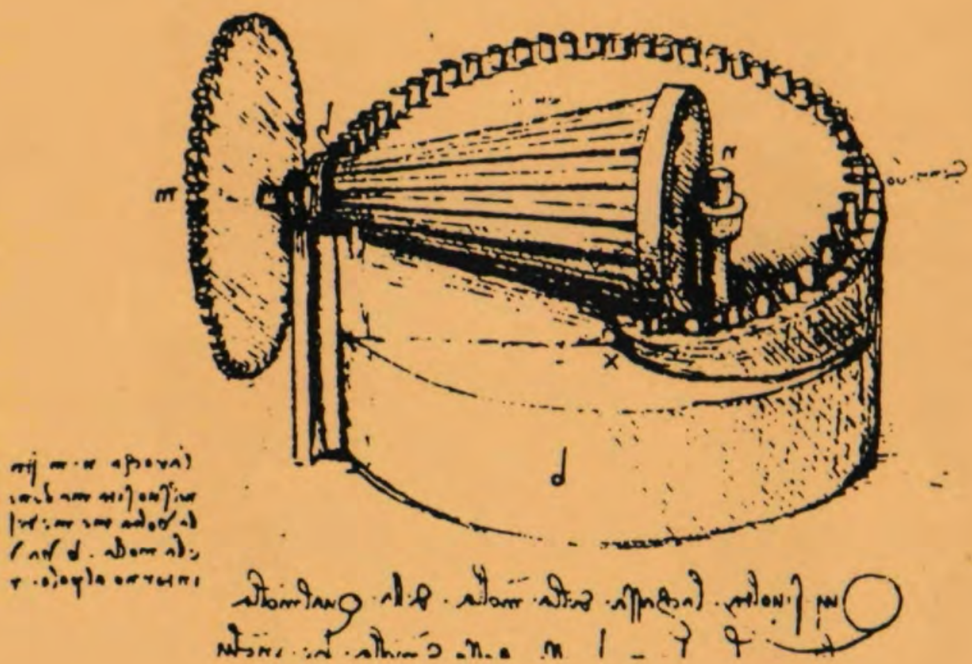

Use of Boundary Elements for Determination of the Geometry Factor

Describing Non-Standard Gears

KHV Planetary Gearing—Part II

Relationship of Gear Noise to Gear Transmission Errors

Pfauter & Lorenz.
for any

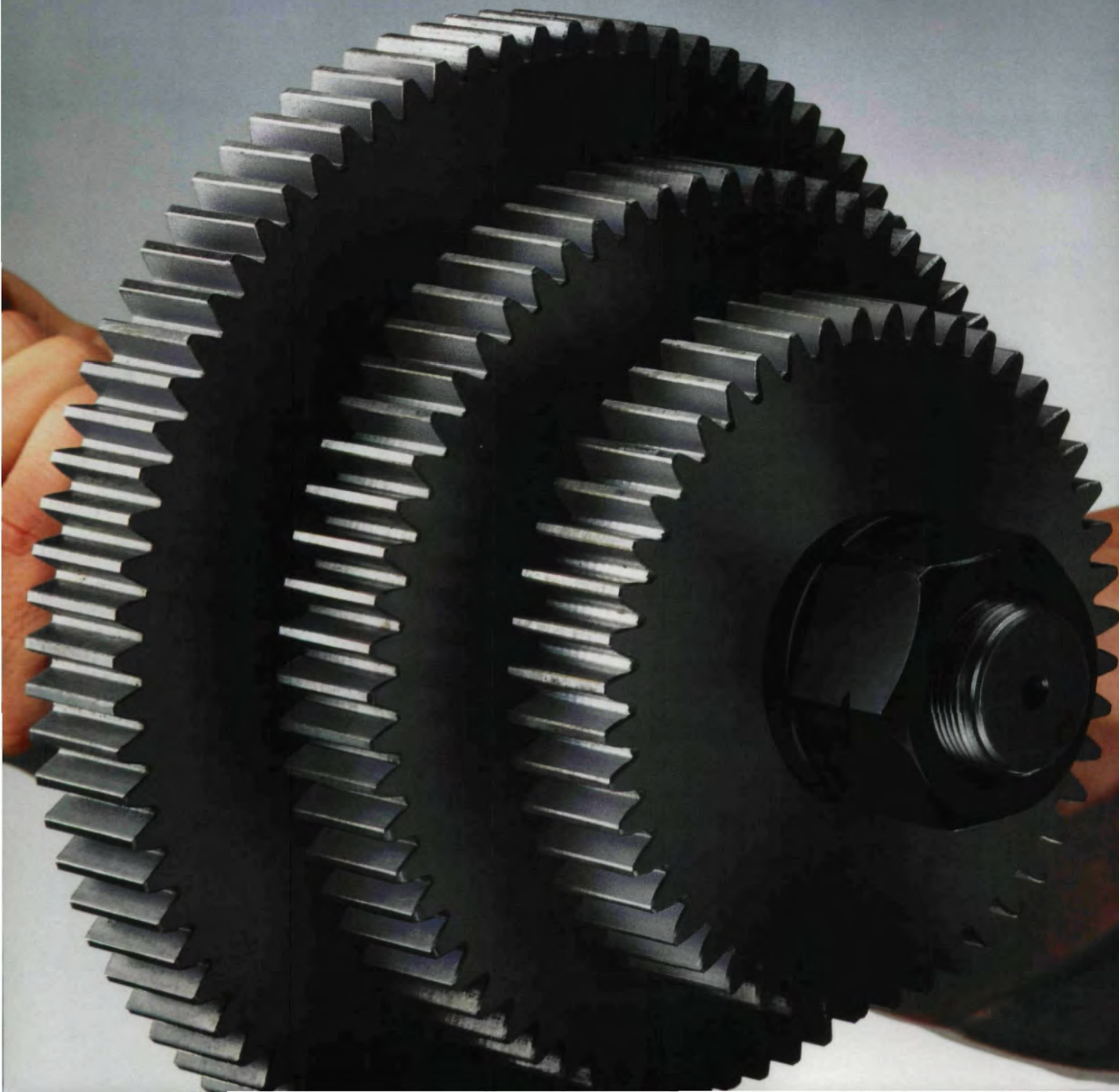


Powerful flexibility
size job.
Pfauter CNC hobbers and Lorenz CNC shapers are used in more gear manufacturing applications than any other CNC machines. Why? Because of their complete flexibility to handle just about any lot size economically.
• Latest generation CNC controls make program preparation and execution an easy task for a single operator.
• Loading/unloading systems are designed to minimize non-productive time.
• Expandable storage capacity substantially increases unattended operation.
• Simple, quick-change tooling increases efficiency.
CAD/CAM designed and built by American Pfauter, these machines have become the reliable standards in aerospace, automotive, truck and tractor, and job shops of every size.
If you'd like to find out how Pfauter and Lorenz CNC technology can improve your productivity, contact American Pfauter, 925 Estes Ave., Elk Grove Village, IL 60007. Phone (312) 640-7500.
AMERICAN PFAUTER
Building American Productivity
member
CIRCLE A-1 ON READER REPLY CARD

We make gear inspection Marvelously Simple with the Simply Marvelous 3000 QC System

Smart™ Probe package. LVDT probe and μprocessor-based convertor deliver high-speed data in μinches.

Operator Control Panel for part loading and machine set up.

Keyboard with "Mouse" for one-time entry of part print and tolerance data. "Mouse" permits use of CAD techniques.

Color graphics CRT with touch screen makes operation simple and fast.

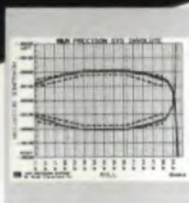

Graphics printer copies CRT.

Plotter delivers multi-color hard copy of graphics and test data.

CNC status monitor provides status and positional display of mechanical system and CNC control functions.

Our Model 3000 QC Gear Analyzer is a third generation CNC gear inspection system incorporating all of the comprehensive analytical tests and evaluation capabilities of previous M & M systems, such as our Model 2000, but with these added capabilities:

- Dramatically improved speed and accuracy through new mechanical system design and advanced CNC control technology.
- Computer hardware and applications software are modular to allow the user to buy only the required capability. This makes the 3000 QC adaptable to laboratory testing or production-line inspection.
- Integrated Statistical Process Control with local data base capability is an optional feature.
- Networking with MAPS compatibility is available.
- Robotic interfacing for totally automatic load/test/unload operation can be incorporated.

For more information or applications assistance, write or call: M & M Precision Systems, 300 Progress Rd., West Carrollton, OH 45449, 513/859-8273, TWX 810/450-2626, FAX 513/859-4452.

M&M PRECISION SYSTEMS

AN ACME-CLEVELAND COMPANY

CIRCLE A-6 ON READER REPLY CARD

GEAR TECHNOLOGY

The Journal of Gear Manufacturing

RANDALL PUBLISHING
1401 Lunt Avenue
P.O. Box 1426
Elk Grove, IL 60007
(312) 437-6604

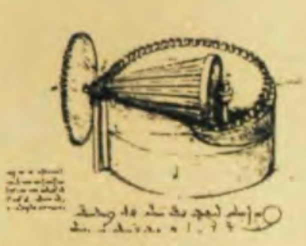

The Advanced Technology of Leonardo Da Vinci 1452-1519

COVER

Like all engineers, Leonardo had his failures as well as his successes. The illustration on this issue's cover shows a tentative solution to the problem of equalizing the force of the clock spring in a timekeeping device. In the sketch Leonardo experiments with the idea of placing a volute gear on the spring barrel and in mesh with a sliding pinion guided by the edge of the volute. The design problem here is that the straight guide on the side of the pinion would interfere on the inside curve of the volute. This interference would increase as the center of the volute was approached.

CONTENTS — PAGE NO.

FEATURES

DEPARTMENTS

January/February, 1988 — Vol. 5, No. 1

GEAR TECHNOLOGY, The Journal of Gear Manufacturing (ISSN 0743-6858) is published bimonthly by Randall Publishing Co., Inc., 1425 Lunt Avenue, P. O. Box 1426, Elk Grove Village, IL 60007. GEAR TECHNOLOGY, The Journal of Gear Manufacturing is distributed free of charge to qualified individuals and firms in the gear manufacturing industry. Subscription rates for non-qualified individuals and firms are: $35.00 in the United States, $55.00 for foreign countries. Second-Class postage paid at Arlington Heights, IL and at additional mailing office.
Postmaster: Send address changes to GEAR TECHNOLOGY, The Journal of Gear Manufacturing, 1425 Lunt Avenue, P. O. Box 1426, Elk Grove Village, IL 60007.

MANUSCRIPTS: We are requesting technical papers with an educational emphasis for anyone having anything to do with the design, manufacture, testing or processing of gears. Subjects sought are solutions to specific problems, explanations of new technology, techniques, designs, processes, and alternative manufacturing methods. These can range from the "How to . . ." of gear cutting (BACK TO BASICS) to the most advanced technology. All manuscripts submitted will be carefully considered. However, the Publisher assumes no responsibility for the safety or return of manuscripts. Manuscripts must be accompanied by a self-addressed, self-stamped envelope, and be sent to GEAR TECHNOLOGY, The Journal of Gear Manufacturing, P.O. Box 1426, Elk Grove, IL 60007, (312) 437-6604.

GENIUS

CIMA USA's CE350 *CNC6.*

At CIMA USA, the legacy of Da Vinci inspires us every day. Because we share his Italian heritage—CIMA is Europe's leading producer of gear hobbing equipment. Because we admire the fact that he applied his creativity to questions long before anyone else thought to ask them.

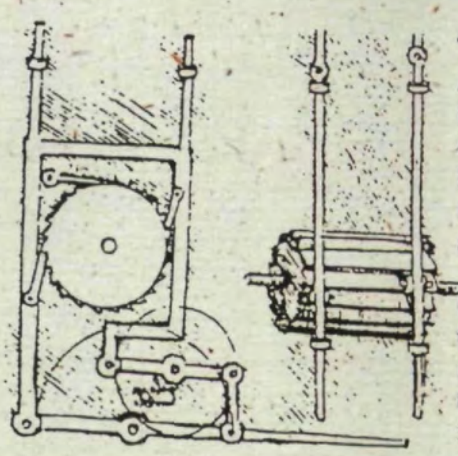

Da Vinci was fascinated with gears and motion.

The Genius of CIMA.
At CIMA USA, our genius is answering your questions with adaptations customized to your gear manufacturing needs. We think the best solutions make your operation more productive and more profitable.

Only CIMA offers four different CNC control configurations, all manufacture software integrated for maximum speed in data interpolation. CIMA has the only Flexible Machining Systems in the world, custom-

Leonardo Da Vinci.

His genius was inventing imaginative answers to human problems, using science and intuition. His incredible curiosity and intellect produced designs which were centuries ahead of their time.

CIMA USA's CE220 *CNC6.*

assembling CIMA components for your specific manufacturing demands.

The Real Genius: You.
Da Vinci was adept at listening to the concerns of people around him. CIMA USA's brightest idea is simply listening to you.

The CE220 and CE350 gear hobbing machines are two of CIMA's key building blocks for custom solutions. And we've made them completely flexible so they can be adapted to a wide range of needs.

CIMA Genius, American Style.
Now, all of CIMA USA's equipment is built in our American factory to your American standard. That lowers costs to you up front, and makes service and spare parts more accessible down the road.

And CIMA USA gear hobbing machines still trim set up time, speed up tool changes and provide greater cutting accuracy. Which gives you productivity that even Leonardo Da Vinci would have admired.

Circle us on the reader card for more information. Or, better yet, call today and tell us exactly what your needs are. Because when you and CIMA USA get together, it's powerful. That's genius!

CIMA USA
Putting Powerful Ideas In Gear.

Division of G.D. P.M., Inc.
501 Southlake Boulevard
Richmond, Virginia 23236
(804) 794-9764
Telefax (804) 794-6187 • Telex 648-4252

EDITORIAL

THE SEEDS OF OUR FUTURE ARE NOW BEING PLANTED

Mr. Richard Norment, director of AGMA, (left) and Michael Goldstein at Gear Expo '88.

A medieval philospher once said that if he knew for certain the world was to end tomorrow, he would be sure to take time to plant an apple tree in his garden today. The recent events in the world financial capitals have seemed a bit like prior notice of something cataclysmic, but like the philosopher, we can still find some reasons for hope in the face of an uncertain future. The good news for our industry is that four important efforts on the part of various organizations promise to have long-term positive effects on both the gear and machine tool businesses.

First, the October AGMA Gear Expo '88 and Fall Technical Conference held in Cincinnati got very positive reviews from nearly everyone. "Not as good as we'd like it to be, but much better than we thought . . . I'll definitely be back in two years!" That seems to be the over-all consensus of the exhibitors and the 1200 attendees from 15 foreign countries.

The number and quality of the exhibitors was a pleasant surprise to many. We saw more suppliers with more machines than anticipated. Certainly the early commitment by Hagen Hoffman of BHS Hofler to exhibit a large operating grinder and major machine tool exhibitions by National Broach and Mitsubishi, helped to anchor the more than 100 booths of smaller machine tools, test equipment, cutting tools, software, other products and services.

The atmosphere of the show and the setting of Cincinnati was especially conducive to a successful undertaking. As a first-time exhibitor, we were pleased to know that every one of the attendees either knew us personally or at least had heard of GEAR TECHNOLOGY. A big plus in the minds of many exhibitors was the knowledge that virtually everyone they talked to was a potential customer. There was a feeling that the people who attended had come to do business.

The facilities were excellent and convenient to the hotels. The city of Cincinnati was beautiful, especially at this time of the year, and the nice weather made it a pleasure. The informal quality of the city and the continuous programs somewhat precluded lavish entertaining by some exhibitors, "leveling the playing field" for everyone and fostering a spirit of pleasant comeraderie. Technology, productivity, products, services, personal relationships and commitments were the driving force in Cincinnati.

The technical conference was every bit as good as the show. The quality of the papers was the best I've seen in years. You will be seeing some of these articles in the coming issues.

All around, I think everyone has deemed Cincinnati a huge success for what was really a first-time effort. Those of you who missed Cincinnati, either as an attendee or an exhibitor, missed something special and should not make the same mistake in 1989. The next Expo in 1989 promises to be even more exciting than this one, and an even larger turn-out should be anticipated.

Shortly after Cincinnati, SME held its successful Gear Processing and Manufacturing Clinic in Detroit. Some 130 people heard 25 papers on gear related subjects. Two especially popular features of this year's conference were the panel discussions at the end of each day and the open forum on the last evening of the conference. These gatherings gave the audience an opportunity to share concerns and questions and talk one-on-one with the presenters, and they are a welcome addition to the SME program.

(continued on page 37)

The Use of Boundary Elements For The Determination of The AGMA Geometry Factor

Sandeep M. Vijayakar
Donald R. Houser
The Ohio State University
Columbus, Ohio

Abstract:

The traditional method of computing the geometry factor has limitations in its consideration of internal gears, gears with thin rims or gears with rims having complexities such as spokes and holes. The finite element method may be used in such instances, but is often time consuming for both model development and computation. The boundary element method described in this article, provides an alternative which is easier to set up and allows one to compute geometry factors for many tooth configurations. The examples shown in this article use the boundary element method to show how the peak stress amplitude and its location change with different rim thickness and support conditions.

Introduction

The geometry factor, which is a fundamental part of the AGMA strength rating of gears, is currently computed using the Lewis parabola which allows computation of the Lewis form factor.[1] The geometry factor is obtained from this Lewis factor by applying a stress correction factor, a helical overlap factor and load sharing ratio. This method, which originally required graphical construction methods and more recently has been computerized, works reasonably well for external gears with thick rims.[2-6] However, when thin rims are encountered or when evaluating the strength of internal gears, the AGMA method cannot be used. When these situations are encountered, most investigators have used finite elements to determine the maximum tooth root stresses. Examples of such analyses for thin rimmed gears are presented by Drago,[7,8], Suzuki et al,[9] Chong and Kubo[10] and Eloranta.[11] Castellani and Castelli[12] compare both AGMA and ISO rating methods with finite element results. In addition, Chong et al[13,14] have developed an approximate formula for the analysis of thin rimmed gears. Ishida et al[15,16] and Drago[17] present measured stress data for thin rimmed gears. The state of stress for internal gears has been analyzed by numerous investigators.[18-24]

The previous investigators have shown that the assumptions of the AGMA method for thin rimmed gears and for internal gears cannot be used successfully. The finite element method is viable, but because of time consuming procedures in creating a model and in handling unusual boundary shapes, it can be quite burdensome and will usually require considerable computer power, even for two dimensional elements. An analysis procedure which shows promise, both from a model building standpoint and from computational efficiency, is the boundary element method.[25,26] This *method, which has some of the features of the finite element* method, has been applied to gears by Gakwaya et al.[27] Rubenchik[28] used a similar method called the boundary integral method for the computation of root stresses. The paper by Oda et al,[31] etc. which appeared at the same time that this article was being prepared, carries out an extensive comparison between the stresses at the roots of thin rimmed external and internal gears by the boundary element method, the finite element method and from experiments. Since the boundary element method potentially can be used on personal computers and models can be easily developed, this article presents an introductory study of its potential in computing geometry factors.

Subsequent sections of this article outline the fundamental theory of the boundary element method and present some preliminary results. The computational procedure is such that

---

AUTHORS:

DR. SANDEEP M. VIJAYAKAR *received his B'Tech degree from the Indian Institute of Technology at Bombay and his M.S. and Ph.D. from Ohio State University. He is currently a research associate at Ohio State and a member of ASME.*

DR. DONALD R. HOUSER *is on the faculty of the Department of Mechanical Engineering, Ohio State University. In addition to his teaching responsibilities, he has researched and published in the areas of gear dynamics and noise, v-belts, vibration diagnostics and vibration signal analysis. He is also currently director of the university's Gear Dynamics and Gear Noise Research Laboratory. Dr. Houser is a member of ASME, SAE, AGMA and Tau Beta Pi, Pi Tau Sigma and Sigma Xi honorary fraternities. He is also chairman of the ASME Power Transmission and Gearing Committee. Dr. Houser received his degrees in mechanical engineering from the University of Wisconsin at Madison.*

the geometry factor is directly determined so that it may be used in the current AGMA 218.01 rating standard. Since the AGMA method currently in use is a two-dimensional analysis method, the authors decided to use a two-dimensional boundary element. Note, however, that in many complex root stress problems, three-dimensional analyses should be used in order to obtain accurate stress results. Gakwaya et al[27] show comparisons of the computational time required by the boundary element method and the finite element method. Holze[29] discusses advantages and disadvantages of the boundary integral equation method and compares it with the finite element method for a plane-stress gear-tooth problem.

Boundary Element and Finite Element Methods

The finite element method divides the body that is being studied into many pieces or elements whose behavior is easier to approximate than that of the whole body. The equations describing each element are "assembled" in a system of linear equations and are then solved.

The boundary element method, on the other hand, does not divide the body under consideration into elements. For a homogenous, isotropic body with no body forces, the only causes for displacements and stresses within the body are loads and displacements applied along the boundary. The body can be considered to be part of an infinitely extending material which is subjected to loads along the original boundary. Thus, if a function which describes the response of an infinitely extending medium to a point load is known, then this function can be used to compute the response of the body by moving the point load along the boundary and integrating each individual response. Therefore, the integration which is carried out numerically by breaking the boundary into elements only needs to be carried out along the boundary. The boundary element method has the advantage of not requiring that the interior of the body be divided into two-dimensional elements with only the boundary being divided into one-dimensional elements. Because of its mathematical complexity and because other references, such as Brebbia,[25] provide the mathematical details of the boundary element method, its theoretical basis is not presented in this article. However, a summary of its theory is presented in the Appendix.

An important advantage of the boundary element method is that it is usually able to represent areas of stress concentration and singularities better than general purpose finite element methods. Because only the boundary needs to be made discrete in boundary element methods, it is possible to work with smaller systems of equations and arrive at very accurate results.

Boundary Element Mesh Generator and Boundary Element Program

The problem of writing a finite element mesh generator which is capable of creating good meshes for all possible types of gear teeth and for many types of shapes is complicated; whereas, writing a boundary element mesh generator is a somewhat simpler task. It is possible to devise a mesh generation scheme that in two dimensions works very well for all kinds of gear teeth with an assortment of shapes.

In the boundary element mesh generator used in the following numerical examples, the only input data required is a description of the hob that is used to cut the gears (or the gear shaper, in the case of the internal gears).

The generator program computes the position and unit normal vectors at a number of points on the hob and uses these values to compute the positions of the corresponding points on the gear by using the conjugacy equations. Fig. 1 shows the hob generating the geometry of a side of a gear tooth. Undercutting is detected numerically. The boundary of the gear tooth is divided into several segments, and the user is asked to input the number of boundary elements into which each segment is to be divided, as shown in Fig. 2.

The meshes generated by this program model three teeth,

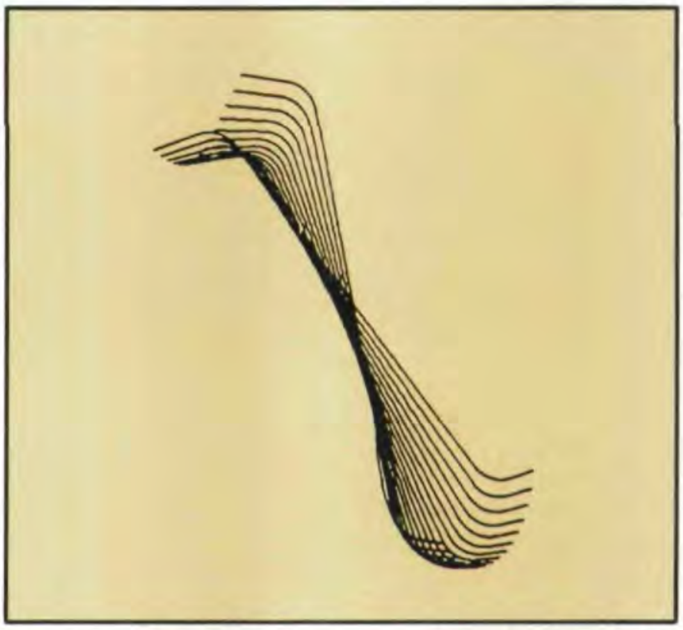

Fig. 1 – The process of generating the gear tooth geometry from the hob geometry.

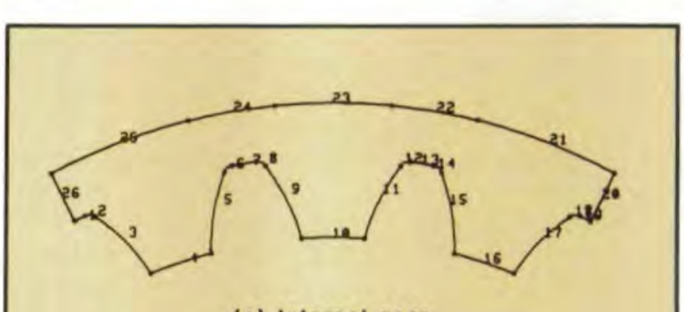

Fig. 2 – Gear tooth boundary and its subdivision into segments.

Table 1. Results of test cases

Mesh	Number of teeth	Radius of inner bore (,outer radius for int. gear)	Ratio of rim thickness to whole tooth depth	Radius at point of max. stress from BEM	J Factor by the BEM	J Factor by the FEM
1	20	0.7"	0.67	0.864"	0.335	0.310
2	20	0.7"	0.67	0.864"	0.343	0.319
3	20	0.8"	0.25	0.856"	0.159	0.135
4	20	0.8"	0.25	0.876"	0.389	0.356
5	20	0.95",1.2"	0.67	1.100"	0.123	–
6	20	0.95",1.2"	0.67	1.100"	0.412	–
7	12	0.3"	0.67	0.478"	0.255	–

with the load being applied on the center tooth. Three teeth are used to accurately model the effects of rim thickness and of boundary conditions on the root stresses. The current program provides two means of constraining the model, the first being to fix all sides of the tooth support, and the other being to fix only the ends of the rim and to leave the inner bore free. Other possible ways of constraining the teeth that are to be implemented in the future include roller and contact type boundary conditions. The mesh that is generated can be modified to account for features such as keyways and weight reducing holes. It was found advisable not to make the mesh too coarse at the point of load application or at the supports.

The user is given a choice of either specifying the radius at which a unit normal load is applied on the involute part of the profile, or letting the program compute the highest point of single tooth contact and applying the load there. The user is also given the choice between plane strain and plane stress conditions for the gear tooth model. The choice between these two conditions depends on how wide the gear tooth is in relation to its other dimensions.[30]

The meshes generated by the above mentioned mesh generator are sent to a general two-dimensional boundary element program written by the authors. The boundary element method does not allow computation of stresses on the boundary because of the numerical behavior of the fundamental solution, which imposes a restriction similar to the finite element method, where one computes stresses only at Gauss points. This program computes the displacements of the nodes of the mesh and then searches along the boundary for the maximum stress at the boundary. Stresses at the boundary are calculated by computing stresses at both one element length and one-half element length from the boundary and then extrapolating stresses to the boundary. The multi-axial state of stress at all points is converted into an effective stress using one of the many available multi-axial theories of failure. In the numerical examples that follow, the maximum principal stress is used as the failure criterion.

Table 2. Dimensions of the Hob used to Cut the External Gears used in the Test Cases.

Diametral pitch	10.0
Pressure angle of the rack	20°
Addendum constant of hob	1.4
Dedendum constant of hob	1.0
Corner radius at tip of the hob tooth	0.02 in
Fillet radius at root of the hob tooth	0.02 in

As per the defining equation of the J factor in the AGMA standard 218.01,[1]

$$s_t = \frac{(K_a K_s K_m)}{K_v} \left(\frac{W_t P_d}{F\,J}\right)$$

where

- K_a is the application factor,
- K_s is the size factor,
- K_m is the load distribution factor,
- K_v is the dynamic factor,
- F is the face width,
- W_t is the transmitted load,
- P_d is the diametral pitch and
- J is the geometry factor.

The stress s_{BEM} that the boundary element method computes includes the effect of the geometry that the J factor represents, but does not include the effects of the application, size, load distribution and dynamic factors. Therefore,

$$s_{BEM} = \left(\frac{W_t\, P_d}{F\,J}\right)$$

so that the J factor can be computed from the stress value s_{BEM}.

Numerical Examples

Table 1 describes the seven gears used for the numerical examples, and Table 2 gives the geometery of the hob that was used for all the external gears. Mesh 1 (Fig. 3) is a thick rimmed gear, whose rim is not constrained, and Mesh 2 (Fig. 4) is the same gear, whose rim is constrained. The location

(continued on page 33)

Describing Nonstandard Gears — An Alternative to the Rack Shift Coefficient

Donald R. McVittie
Gear Engineers, Inc.
Seattle, WA

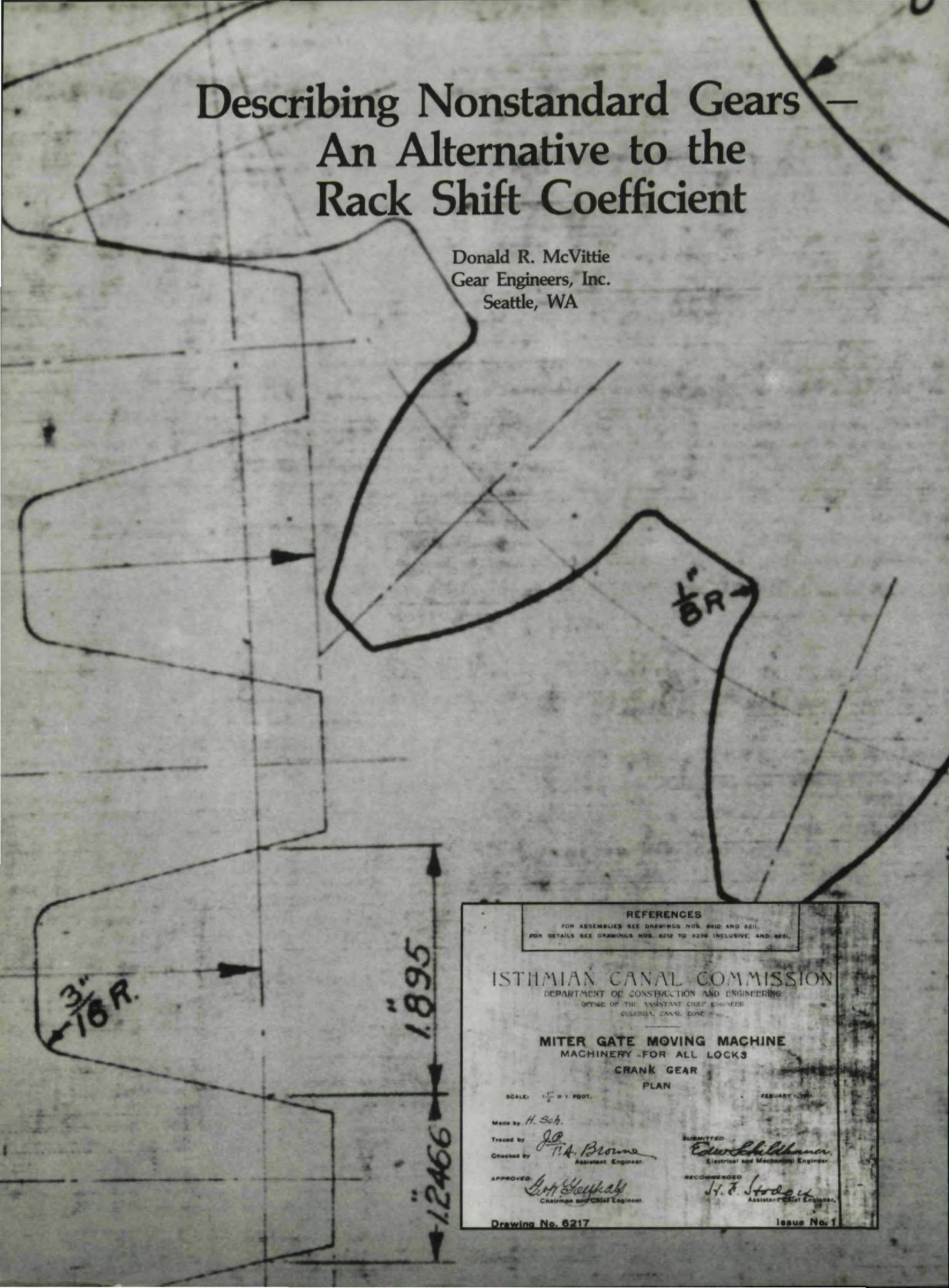

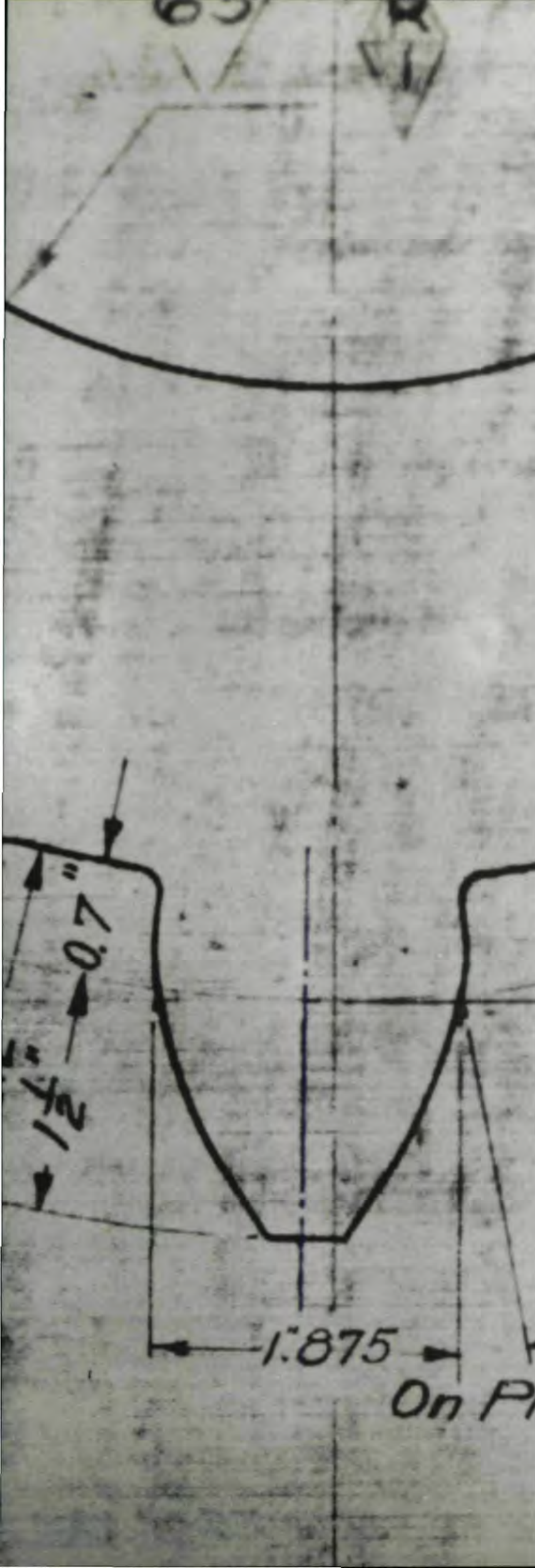

Abstract

The rack shift method of describing gears made with nonstandard addendum diameters (tip diameters or nonstandard tooth thickness) has serious limitations, since the nominal pitch of the cutting tool, which is required for the calculation of rack shift coefficient, may not be available to the designer, may vary as the tool is sharpened or may be different for the gear and its mate.

The details of the calculation of rack shift coefficient are not standardized, so there is little agreement between analysts about the value of "x" for a given nonstandard gear or gear pair. Two common methods to calculate rack shift coefficient are described in this article.

This article proposes a different nomenclature for nonstandard gears, using the involute function of the transverse pressure angle at the diameter where the space width is equal to the circular tooth thickness. This is calculated from the fundamental relationships between number of teeth, normal base pitch, axial pitch and normal base tooth thickness.

This dimensionless value, called "T", is used with the addendum diameter and face width to describe a single gear. A pair of gears is described by the same system, by adding center distance and backlash to the parameters.

Introduction

The use of dimensionless factors to describe gear tooth geometry seems to have a strong appeal to gear engineers. The stress factors I and J, for instance, are well established in AGMA literature. The use of the rack shift coefficient "x" to describe nonstandard gear proportions is common in Europe, but is not as commonly used in the United States. When it is encountered in the European literature or in the operating manuals for imported machine tools, it can be a source of confusion to the American engineer.

Even those who use the rack shift method do not agree on how to evaluate the rack shift coefficient of a specific gear set. As a test, the author sent a set of data for a simple spur gear set to seven gear engineers in the U.S. and Europe with the request that they evaluate the "x" factor. Of the six replies, no two results were the same! The value of the rack shift coefficient "x" varied by more than 20%. The gear data and the results are tabulated in Appendix C.

This article proposes that these nonstandard gears be described by a different parameter, the involute function of

AUTHOR:

DONALD R. McVITTIE is president of Gear Engineers, Inc., Seattle, WA, a professional engineering company specializing in gear design, analysis and gear capacity studies. He is also director and member of the underwriting and claims committee for GMI, Ltd., a product liability insurance company owned by a group of gear manufacturers. He was Executive Vice President of The Gear Works-Seattle, Inc. until his retirement in 1986.

A graduate of University of Michigan with a degree in mechanical engineering, Mr. McVittie is an active member of AGMA, where he is Vice President of the Technical Division. He was AGMA president in 1984/85. He is a licensed professional engineer in the State of Washington, and member of ASME, SNAME and SAE and the author of several technical papers.

the transverse pressure angle where the tooth thickness equals the space width.

Before describing the proposal, the rack shift method of describing nonstandard involute gears and some of its limitations are discussed.

Rack Shift Coefficient – Two Definitions

Outside Diameter Method. One definition of rack shift coefficient is given by Maag:[1]

"The amount of the radial displacement of the datum line from the position touching the reference circle is termed *addendum modification*. This amount is given a positive sign in the calculations when the displacement is away from the center of the gear, and a negative sign when towards the center of the gear. . . The *addendum modification coefficient* $\underline{x}$ is the amount of addendum modification measured in terms of the diametral pitch or module.

$$\text{Addendum Modification} = \frac{x}{p} \text{ (or x.m)} \qquad (1)$$

The dimensions of the gears can be determined as the so-called zero backlash gearing by means of a system of equations. (In practice the backlash is obtained by the tolerances on the theoretical, nominal dimension.)"

This definition, which will be called the outside diameter (OD) method, is useful because, if root clearances are kept standard, the center distance can easily be calculated without confusing the calculation with considerations of operating backlash. (See Figs. 1 & 2.) It is clear that, even without using a dimensionless coefficient

$$C = \frac{D_{o1} + D_{r2}}{2} + c \qquad (2)$$

where

D_{o1} = Outside diameter of pinion
D_{r2} = Root diameter of gear
C = Center distance
c = Root clearance.

The geometry is calculated as if the gear were cut by feeding a hob in from the outside diameter to standard depth, then side cutting to achieve the desired backlash.

The gear data block includes "backlash allowance in this gear", which specifies the amount of this side cutting. For gears which are to run on widely spread centers, this backlash

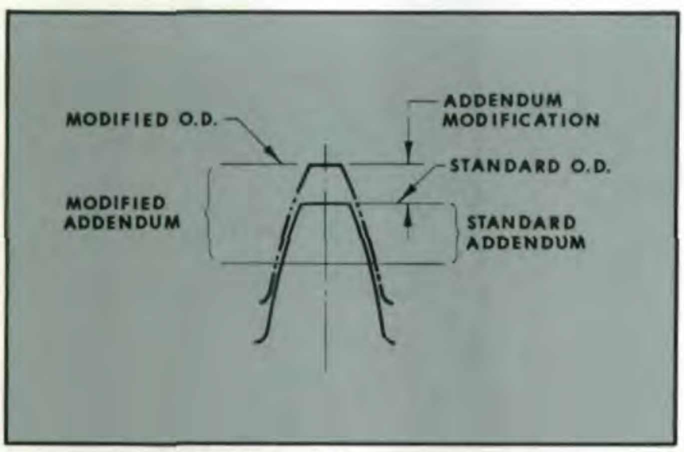

Fig. 1 – The outside diameter method.

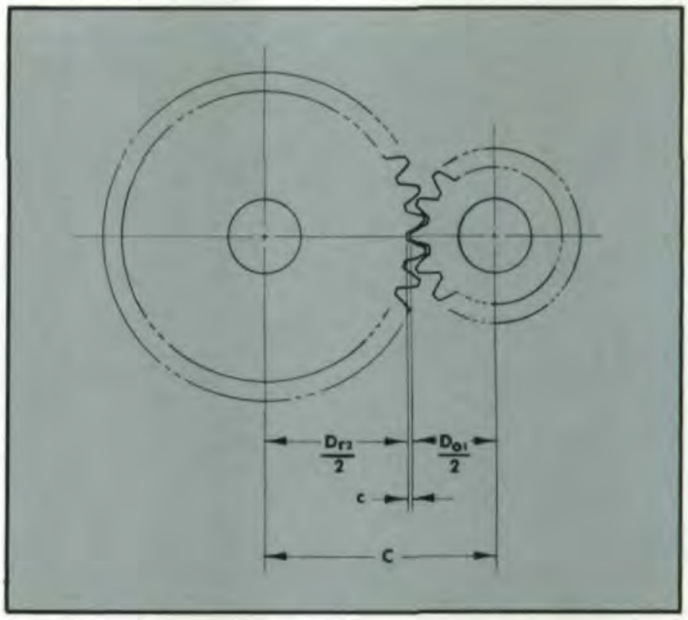

Fig. 2 – Center distance using constant radial clearance.

allowance must be negative to provide reasonable operating backlash. Negative backlash allowance is a difficult concept which can lead to false expectations of root clearance.

This is a simple mathematical convention, but it is not the way gears are made. In real life, the cutter is fed in until the desired tooth thickness is achieved. The resulting root diameters are not the same as those assumed in the original convention, so the root clearances on which the convention is based are not standard.

Nonstandard root clearances are not much of a problem if they are greater than expected, but they can lead to interference problems in those gears which have negative "backlash allowance" in order to operate properly on spread centers. (See Fig. 3.)

The interference can be alleviated by reducing the outside diameter to restore the standard clearance, but this throws the engineer into a loop, since the x factor is based on the OD. Lorenz[2] introduces a K factor (tip modification factor) to clean this up without recalculating the x factor.

This definition has a more subtle problem, since helical gears and spur gears with the same normal generating tooth thicknesses do not have the same x factor, even though it seems they should. This question will be covered later in this article.

Tooth Thickness Method. Another definition of rack shift is related to the actual position of the cutting tool when cutting the thickest allowable teeth for the design under consideration.

$$x = \frac{(P_{nd}t_{sn} - \pi/2)}{2 \tan \phi_c} \qquad (3)$$

where

t_{sn} = Tooth thickness at standard (generating) pitch diameter.
P_{nd} = Normal diametral pitch
ϕ_c = Cutter profile angle

This is dimensionless, since the tooth thickness is multiplied by the diametral pitch or divided by the module. We shall call this the tooth thickness (TT) method. (See Fig. 4)

The TT method eliminates the problems with negative backlash allowance and misleading root clearance assumptions inherent in the OD method. It offers little help in calculating center distance if tooth thicknesses are known, or in calculating tooth thicknesses to operate at a specified center distance. In this method, the outside diameters of the gears are calculated from the center distance, the root diameters and the required root clearances.

$$D_{o1} = 2(C - c) - D_{r2} \qquad (4)$$

If two gears are operated on a center distance equal to the sum of their standard pitch radii plus the sum of their rack shifts calculated by the TT method, the operating backlash will vary in a complex manner with the sum of the rack shifts. Backlash is zero when the sum of rack shifts is zero, but it must be calculated from operating pitch diameters and operating tooth thicknesses when the sum of rack shifts is not zero. The time required to perform this lengthy iterative process usually precludes the development of an optimum design.

Most of those who responded to the sample problem assumed a "backlash allowance" and adjusted the tooth thicknesses arbitrarily to define a hypothetical "zero backlash set". The differences in their assumptions account for some of the differences in their calculated "x" factors.

Cutter Standards and Standard Racks. In order to make any of the definitions of rack shift dimensionless, the designer must assume a cutter diametral pitch or module. This is usually done in terms of a hypothetical standard rack by assuming that the rack geometry is "standard" where the tooth thickness and the space width of the rack are equal to one half of the rack's circular pitch.

This is dangerous ground. Tool designers and gear machines operate with base pitch, regardless of what is marked on the end of the tool. Short pitch hobs, single tooth rack shaper cutters, single tooth grinders and two wheel grinders are

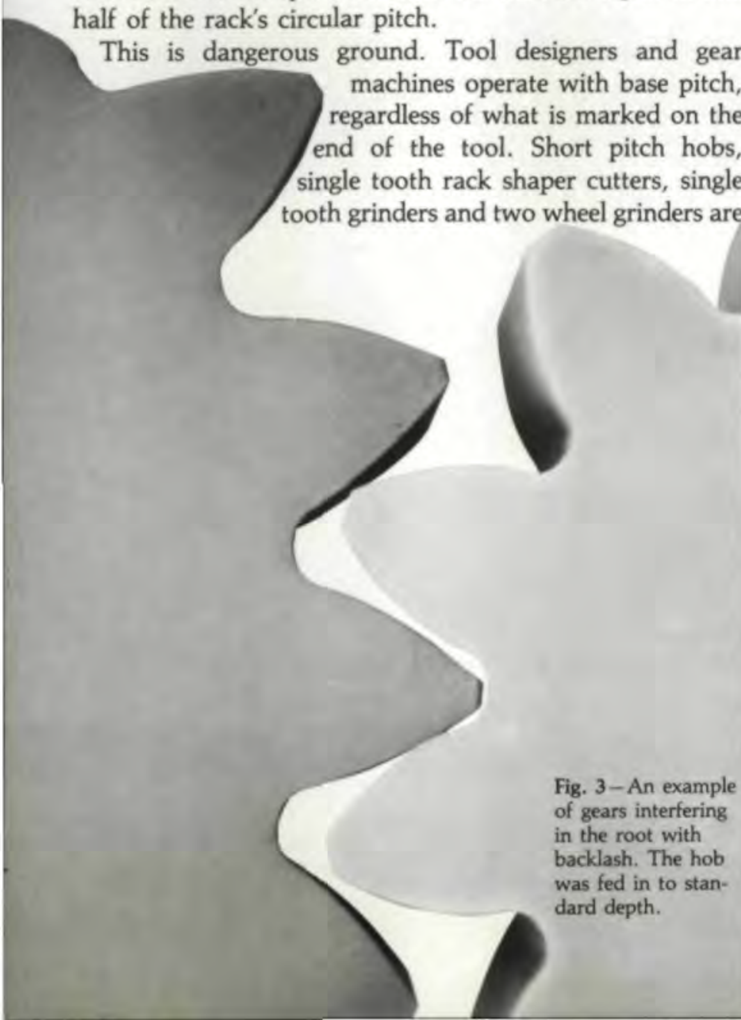

Fig. 3—An example of gears interfering in the root with backlash. The hob was fed in to standard depth.

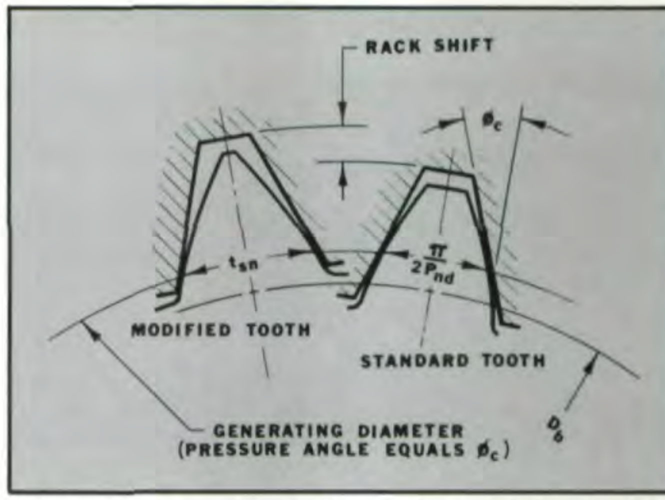

Fig. 4—Addendum modification factor by the tooth thickness method.

beyond standardization by the "half circular pitch" method.

What is the designer to do? Usually an assumption is made by the designer and ignored by the manufacturing department. The result can be a surprise, usually discovered on the assembly floor.

Earlier Publications

Finding an easy way to calculate the dimensions of nonstandard gears has been the subject of countless papers and articles. As early as 1911, the Isthmian (Panama) Canal Commission[3] used 1 DP oversize spur pinions in the gate mechanisms for the Gatun and Miraflores locks. These gears were made on special Gleason gear planers from a layout, another method which is hard to describe in terms of a standard rack form.

As the advantages of nonstandard gears became better recognized, many authors tried to develop systems for "standardized" nonstandard systems. Maag offers pages of charts, nomographs and advice on this subject. An interesting paper by Grosser[4] provides eight pages of charts to help with these calculations. Farrel[5] also provides guidance in selecting the proportions of gears intended to operate on spread centers. Most of this work dates from the days of mechanical calculators and tables of logarithms, when the difficulty of finding the value of an angle from its involute function was avoided whenever possible to save calculation time.

Computers and the Inverse Involute

Today we can find the arc involute as easily as we find the arc cosine. Even pocket calculators are easily programmed to give an accurate result. There are many algorithms. Cooper[6], Errichello[7] and Laskin[8] all work and are readily available. Easy access to the arc involute frees us up to optimize nonstandard gears if we can find a more direct way to calculate center distance, backlash and limit diameters from tooth thicknesses, or vice versa.

Summary of This Article

This article will demonstrate that the involute function of the transverse pressure angle, where the tooth thickness is equal to the space width, called the "T" factor, is a useful way to describe nonstandard gears. With this parameter, a series of simple equations can be developed, which simplify nonstandard gear geometry calculations and reduce iteration. The "T" factor is

- Dimensionless
- Easily calculated
- Independent of helix angle
- Independent of the cutter geometry
- Independent of the mating gear
- Unique for the geometry of the gear described.

Nomenclature and Definitions

Definitions. Symbols are defined where they are first used in this article. For convenience, a list of symbols is provided in Table 1.

The subscript "1" refers to the pinion, and the subscript "2" refers to the gear.

Fundamental Parameters of the Involute Tooth Form

The involute portions of a meshing gear pair can be completely described in terms of a short list of fundamental parameters.

Numbers of Teeth. The number of teeth on each gear must be known before the geometry can be defined.

Base Pitch. The base pitch must be determined from the cutting tool or arbitrarily if the gear is to be made on a machine where base pitch is adjustable. Base pitch can be measured in the normal plane or the plane of rotation.

Axial Pitch. Axial pitch, which determines the helix angles of the gear set, is required to define the geometry.

Base Tooth Thickness. Base tooth thickness, which determines all of the tooth thicknesses of a gear, must be established for each gear. Base tooth thicknesses can be measured in the normal or transverse plane.

Center Distance and Backlash. If both base tooth thicknesses of a gear pair are known, either center distance or backlash is required. The other can be calculated. If three of the four; t_{b1}, t_{b2}, C and B, are known, the fourth can be calculated.

Blank Dimensions. The outside diameters of the gear blanks are usually determined by the involute geometry chosen, the cutter addendum and the root clearances desired. They are required, along with the face widths, to completely define the gear geometry.

Root Fillet Geometry. The root trochoidal form is determined by the cutting conditions. It is beyond the scope of this article, since it does not affect the involute portion of the teeth, but it is fundamental to the strength of the teeth. For good control, the root fillet coordinates or the cutting method and cutter form must be specified.

Table 1 — Nomenclature

Symbol	Description	Where First Used
B	Backlash in the plane of rotation	Eq. 5
B_N	Backlash normal to involute profile	Eq. 7
C	Center distance	Eq. 2
c	Root clearance	Eq. 2
D_b	Base circle diameter	Eq. 5
D_{o1}	Outside diameter of pinion	Eq. 2
D_{r2}	Root diameter of gear	Eq. 2
m	*Metric module*	Eq. 1
N_1	Number of teeth in pinion	Eq. 6
N_2	Number of teeth in gear	Eq. 6
P	Diametral pitch	Eq. 1
P_{nd}	Normal diametral pitch	Eq. 3
p	Transverse circular pitch	Eq. 14
p_b	Transverse base pitch	Eq. 5
p_N	Normal base pitch	Eq. 7
p_x	Axial pitch	Eq. 9
T	*Tooth thickness factor (inv ϕ_1)*	Eq. 15
t	Transverse tooth thickness	Eq. 14
t_b	Transverse base tooth thickness	Eq. 5
t_{bn}	Normal base tooth thickness	Eq. 7
t_{sn}	Tooth thickness at standard (generating) pitch diameter	Eq.. 3
x	Rack shift coefficient	Eq. 1
ϕ	Transverse pressure angle	Eq. 14
ϕ'	Transverse operating pressure angle	Eq. 5
ϕ_1	*Transverse pressure angle where space width equals tooth thickness*	Eq. 13
ϕ_c	Cutter profile angle	Eq. 3
ψ_b	Base helix angle	Eq. 7

A Pair of Gears

Gear designers are usually intersested in a pair of gears in mesh, since, like Adam without Eve, one gear is more ornamental than useful. It can be demonstrated that for two gears in mesh:

$$\text{inv}\ \phi' = \frac{t_{b1} + t_{b2} + B - p_b}{D_{b1} + D_{b2}} \qquad (5)$$

where

ϕ' = Transverse operating pressure angle
t_{b1} = Transverse base tooth thickness of pinion
t_{b2} = Transverse base tooth thickness of gear
p_b = Transverse base pitch = $\pi D_b/N$
B = Backlash measured in the transverse plane and in the plane of action
D_{b1} = Base circle diameter of pinion
D_{b2} = Base circle diameter of gear

(Derivations for Equations 5, 12, 13, 14 and 21 are included in Appendix A.)

For either gear or pinion:

$$D_b = \frac{N\ p_b}{\pi} \qquad (6)$$

where

N = Number of teeth

If Equation 6 is combined with Equation 5 and the result is multiplied by cos ψ_b/cos ψ_b, we have the surprising result:

$$\text{inv}\ \phi' = \frac{\pi\ (t_{bn1} + t_{bn2} + B_N - p_N)}{p_N(N_1 + N_2)} \qquad (7)$$

where

- ψ_b = Base helix angle
- t_{bn} = Normal base tooth thickness of pinion or gear
- p_N = Normal base pitch
- B_N = Normal backlash measured normal to involute profile. This is the backlash which would be measured by a feeler gauge inserted between the teeth.

Equation 7 demonstrates that ϕ' is independent of ψ_b. This implies that as a pair of spur gears are made "more helical" by increasing the helix angle, holding the normal base tooth thickness constant and holding the axes parallel, the center distance increases in inverse proportion to the cosine of the base helix angle and the operating transverse pressure angle remains constant. A similar equation appears in Section 1.35 of Maag for checking the calculation of base tangent length.

The tight mesh condition, as with a cutting tool or a master gear, is a special case where the backlash is zero.

If the center distance is known:

$$\cos\ \phi' = \frac{D_{b1} + D_{b2}}{2C} = \frac{p_N(N_1 + N_2)}{2\pi\ C\ \cos\ \psi_b} \qquad (8)$$

$$\psi_b = \sin^{-1}\left(\frac{p_N}{p_x}\right) \qquad (9)$$

where

p_x = axial pitch.

Note: For spur gears, the base helix angle is zero. The value of $\cos\ \psi_b$ is 1.0. Most computers will accept a very large value of p_x, such as 1.0E+9, without significant error, and eliminate the need for a separate routine for spur gears.

If Equation 7 and Equation 8 are solved for ϕ' and equated:

$$\phi' = \cos^{-1}\left(\frac{p_N(N_1+N_2)}{2\pi\ C\ \cos\ \psi_b}\right) = \text{inv}^{-1}\left(\frac{\pi(t_{bn1}+t_{bn2}+B_N-p_N)}{p_N(N_1+N_2)}\right) \qquad (10)$$

If the cutter and numbers of teeth are fixed, this simplifies to:

$$\phi' = \cos^{-1}\left(\frac{K_1}{2C\ \cos\ \psi_b}\right) = \text{inv}^{-1}\left(\frac{t_{bn1}+t_{bn2}+K_2}{K_1}\right) \qquad (11)$$

where

$$K_1 = \text{a constant, } \frac{p_N(N_1+N_2)}{\pi}$$

$$K_2 = \text{a constant, } B_N - p_N$$

This equation is particularly helpful when a gear set must be designed to fill a given center distance, since the combined effects of increasing tooth thickness and increasing base helix angle (or decreasing axial pitch) are shown in one equation.

Once the sum of the base tooth thicknesses is known, it must be divided between the gear and pinion in accordance with the designer's priorities for balanced strength, sliding velocities and whole depth.

Gear Pairs With Non-Parallel Axes. Equation 7 is derived from the assumption that the axes of rotation of the mating gears are parallel. (The base helix angles are equal.) If this is not the case, as in hobbing, shaving and in spiral gears, a more general relationship must be sought, in which the normal operating circular pitches of the mating parts are equal at the operating pitch diameters, and the sum of the normal operating tooth thicknesses plus the normal backlash is equal to the operating normal circular pitch. This leads to Equation 12, which must be solved by iteration.

$$N_1 \text{inv}\phi'_1 + N_2 \text{inv}\phi'_2 = N_1\left(\frac{t_{b1}}{D_{b1}}\right) + N_2\left(\frac{t_{b2}}{D_{b2}}\right) + \pi\left(\frac{B_N}{p_N}\right) - \pi \qquad (12)$$

It can be seen that if the axes of the gears are parallel, so that the transverse operating pressure angles, ($\phi'_1 = \phi'_2 = \phi'$), and the base helix angles are equal, Equation 12 reduces to Equation 7.

One Gear. It has been shown by Grosser that the pressure angle where the tooth thickness is equal to the space width can be found by

$$\text{inv}\phi_1 = \frac{t_b - .5p_b}{D_b} \qquad (13)$$

where

ϕ_1 = pressure angle where space width equals tooth thickness.

In Grosser's general case:

$$\text{inv}\phi = \frac{t_b - (t/p)p_b}{D_b} \tag{14}$$

where

t = tooth thickness at the diameter where ϕ is measured
p = circular pitch at the same diameter.

The similarity between Equations 5 and 13 has led to a search for a way to express the fundamental proportions of a gear pair in the same terms, as dimensionless ratios of t_b, p_b and N, independent of the cutter geometry or the units of measurement.

"T" Factor

Definition. The author proposes that the involute of the pressure angle in the transverse plane at the diameter where the tooth space is equal to the tooth thickness, be used as the dimensionless comparison factor. This factor, called T, for transverse tooth thickness factor, is dimensionless, easily calculated and extremely useful. It would also be possible to use the pressure angle at this diameter, which is in more familiar units, at the expense of an additional mathematical conversion. This angle will be shown for easy reference in parentheses as (ϕ_T) wherever numerical values for T are shown, for easy reference.

Calculation of T. Equation 13 can be restated by multiplying it by $\cos\psi_b/\cos\psi_b$, in terms of normal tooth thicknesses and normal base pitch, as:

$$T = \text{inv}\phi_1 = \frac{\pi(t_{bn} - .5p_N)}{N^* p_N} \tag{15}$$

This is the most convenient general form, since it is valid for both spur and helical gears.

When two gears are considered, T can be substituted into Equation 7 giving:

$$\text{inv}\phi' = \frac{T_1N_1 + T_2N_2 + \pi(B_N/p_N)}{N_1 + N_2} \tag{16}$$

The term "B_N/p_N" is identical to "B/p_b", so that backlash can be taken in either sense, as long as the value of base pitch is consistent.

Some examples will illustrate the uses of this concept.

Fixed Center Distance Gears. Engineers are often asked to specify a gear set with a specific ratio to mesh at a given center distance and a specified backlash. Usually, the ratio will not fit the center distance with spur gears made to standard proportions and with standard (or available) tooling. The choice, then, is to use oversize spur gears, helical gears or oversize helical gears. The possibilities are endless, and the calculations are repetitive, so the tendency is to use the first reasonable resolution without really considering the alternatives.

A simple calculation procedure using the T factor will be illustrated by a numerical example. In these examples, calculations will be made for theoretical gears, representing the tightest center distance expected and the maximum material condition of the gears.

Consider a 35/23 ratio (1.52174/1) and a 6.500" center distance. Assume that 5 DP 20° (p_N = .5904) tooling is available, and the desired normal backlash is .010".

The author has found that 25° is a reasonable upper limit for the transverse operating pressure angle of sets like this, so calculations will begin there. From Equation 8 ψ_b = 22.311° and from Equation 9 p_x = 1.5552".

Rearranging Equation 16, we get:

$$T_1N_1 + T_2N_2 = \text{inv}\phi'(N_1+N_2) - \pi\left(\frac{B_N}{p_N}\right) \tag{17}$$

With the value of $T_1N_1 + T_2N_2$ known, the distribution of base thickness between the two gears is completely up to the designer's judgment. Some of the options are:

Balanced Sliding. If a balance between approach and recess action is desired, T_1 should be approximately equal to T_2, and

$$T = \frac{\text{inv}\phi'(N_1+N_2) - \pi(B_N/p_N)}{N_1+N_2} = \text{inv}\phi' - \frac{\pi B_N}{p_N(N_1+N_2)} \tag{18}$$

Substituting and solving for T:

$$T = .02905791, \ (\phi_T = 24.7555°)$$

Rearranging Equation 15:

$$t_{bn} = \frac{T\,N\,p_N}{\pi} + .5p_N \tag{19}$$

Substituting, t_{bn} = .4208" for the 23 tooth gear and .4863" for the 35 tooth gear.

The tooth thickness values are converted to the transverse plane, and the tooth thicknesses at the generating diameters are calculated. For standard tooling and standard root clearances, the gear OD's will be 5.558" and 8.247", and the tip lands will be .141" and .145", respectively.

For the pinion, the arc of recess action is 20.5°, and the arc of approach is 20.2°. The sliding velocity at the gear tip is 90 inches per second at 1200 pinion rpm, and at the pinion tip it is 87 inches per second. The complete geometry of this gear set is shown as Example 1 in Appendix B.

Balanced Strength. If balanced strength is the first consideration, a solution must be found by iteration.

For external gears with moderate ratios, the iteration can be shortened by setting the T values in inverse proportion to the numbers of teeth, so that the product T x N is a constant. This is equivalent to setting the base tooth thicknesses equal to each other. (See Equation 15.)

From Equation 17, values for T are .036638 (ϕ_T = 26.6303°) for 23 teeth and .024077 (ϕ_T = 23.3217°) for 35 teeth.

Substituting these values into Equation 19, the base tooth thicknesses are .45356".

The outside diameters are 5.654" and 8.151". The tip lands are .1225" and .1574".

The resulting J factors for bending strength are .511 and .458. The complete geometry of this gear set is shown as Example 2 in Appendix B.

This is only one of an infinite number of possible solutions to the problem. Although it provides a reasonable balance, since the J factors are within 6% of the mean, better balance between the bending strengths can be obtained by increasing one base tooth thickness slightly at the expense of the other. The sum of the base tooth thicknesses must be held constant to maintain the operating backlash.

For moderate gear ratios, base tooth thickness is nearly proportional to root tooth thickness, and bending strength is proportional to the cube of root tooth thickness. In our example, a 2% change (.009") in base tooth thickness will make the difference, since $(1.02)^3 = 1.06$. The resulting J factor is .48 for pinion and gear. The designer must judge if such a small change is really significant to the performance of the finished parts. The complete geometry of this gear set is shown as Example 2A in Appendix B.

A higher strength rating might be obtained by increasing the operating pressure angle at the risk of higher noise and a smaller contact ratio. The T factor system allows these possiblities to be explored with a minimum of repetition, and a clear idea of the effects of each change.

Tight Mesh Center Distance. Once the geometry of the work gear is established, the engineer next usually needs the inspection data. If the work gear is to be inspected by the master gear-test radius method, the operating center distance with the master gear will be required. In this example a master gear with a standard tooth thickness – the space width equal to the tooth thickness at the generating pressure angle – will be used.

T for the master gear is then equal to the involute of the transverse generating pressure angle.

$$T = \text{inv}\ (\sin^{-1}(\frac{\sin\phi_c}{\cos\psi_b})) \tag{20}$$

$$T = .019203,\ (\phi_T = 21.6969°)$$

T for the 35 tooth work gear is .024077, from Example 2.

Substituting the appropriate values in Equation 16, inv ϕ' = .022302 and ϕ' = .3972 radians. From Equation 8, the tight mesh center distance is 6.0583". The complete geometry of this gear set is shown as Example 3 in Appendix B.

Shaper Cutting Conditions. If the gear is to be cut with a pinion shaped cutter, the calculation is done as in the previous example, except that allowance must be made for the sharpening condition of the cutter. The operating center distance with the cutter is necessary for the calculation of interference and form diameters with the shaper cutter. It is usually calculated for two conditions, new cutter and thinnest usable worn cutter.

The base tooth thickness of the cutter can be taken from the cutter drawing or from span measurement of the actual cutter. The second alternative is usually best if a worn cutter is to be used to cut the part.

For example, consider a 71 tooth internal spur gear to be cut with a 20 tooth 3 P_{nd} cutter, to a base tooth thickness of .1460". For the gear, T = .015559, ϕ_T = 20.2787°. T, an involute function, must be positive, so the absolute value of N must be used. In the rest of the calculation, the numbers of internal teeth and internal diameters are considered negative.

The results are shown in Table 2.

Table 2

Cutter Data	New Cutter	Worn Cutter
t_{nb}	.6120"	.5247"
T factor	.019156	.005220
ϕ_T	21.6798°	14.2160°
ϕ'	19.668°	21.8441°
C	8.482"	8.605"
Example No.	4	5

Mesh With A Rack. The T factor system can be used to analyze rack and pinion meshes by assuming that the rack is a gear with a very large number of teeth, such as 9999. This eliminates the computational problems caused by infinite values for t_b, C and N_2. The T factor for the rack is equal to its transverse pressure angle. As an example, we will examine a 33 tooth spur pinion, cut with a 5 P_{nd} 14.5° hob to a base tooth thickness of .4131", in mesh with a special rack. The pinion was designed for a special job requiring low noise and high beam strength. The rack pressure angle of 8° was chosen to minimize separating forces and provide a maximum contact ratio for quiet operation.

The rack circular pitch required to match the pinion base pitch is .6143". T is then the involute function of 8°, or .000914.

This unusual gear set was built for a linear motion device, similar to a planer. (See Figs. 5-7.) It illustrates the ability of the T factor to describe the gear geometry and to facilitate the necessary mesh calculations, even if the two parts are made with widely different cutting tools, as is the case here. The complete geometry of this gear set is shown as Example 6 in Appendix B.

Mesh With A Hob. The T factor as derived is valid for meshes where the axes of rotation of the two members are parallel, but not valid in hobbing or shaping with a rack shaped cutter set in the normal plane. In these cases, it is simple to convert the tool geometry to its equivalent rack in the transverse plane by calculating its transverse pressure angle using Equation 17. For example, the 35 tooth helical gear of Example 2 might be cut with a standard hob with a 20° normal profile angle. The transverse pressure angle of the hob, $\phi_T = 21.6971°$ and $T = .019204$. Example 7 in Appendix B shows the complete geometry of this gear set.

Establishing Root and Outside Diameters. The examples given here establish the root diameters of the gear and pinion from the cutting conditions, using the generating diameter and tooth thickness to establish the cutting position of the cutter, and calculating the tip position of the cutter from the actual cutter geometry. This allows the use of different tools for the gear and pinion if desired. The shaper cutter and hob examples show how this works. The outside diameters are chosen to give standard root clearances from the root diameters of the mating parts, except in the cutting tool examples, where the root clearance with the cutter is zero.

The resulting whole depths vary from standard in order to maintain the designed clearances. This system is not required, but it has the advantage of automatically maintaining equal cutting depths for gear and pinion.

Limit Diameter for Minimum Tip Land. Pinions designed to operate on widely spread centers run the risk of having tip lands which are too small for good operation or for proper heat treatment. An adaptation of the T factor allows a quick approximation of the maximum usable diameter limited by minimum tip land. This approximation is based on the premise that a minimum value for tip land should be $.300''/P_{nd}$.

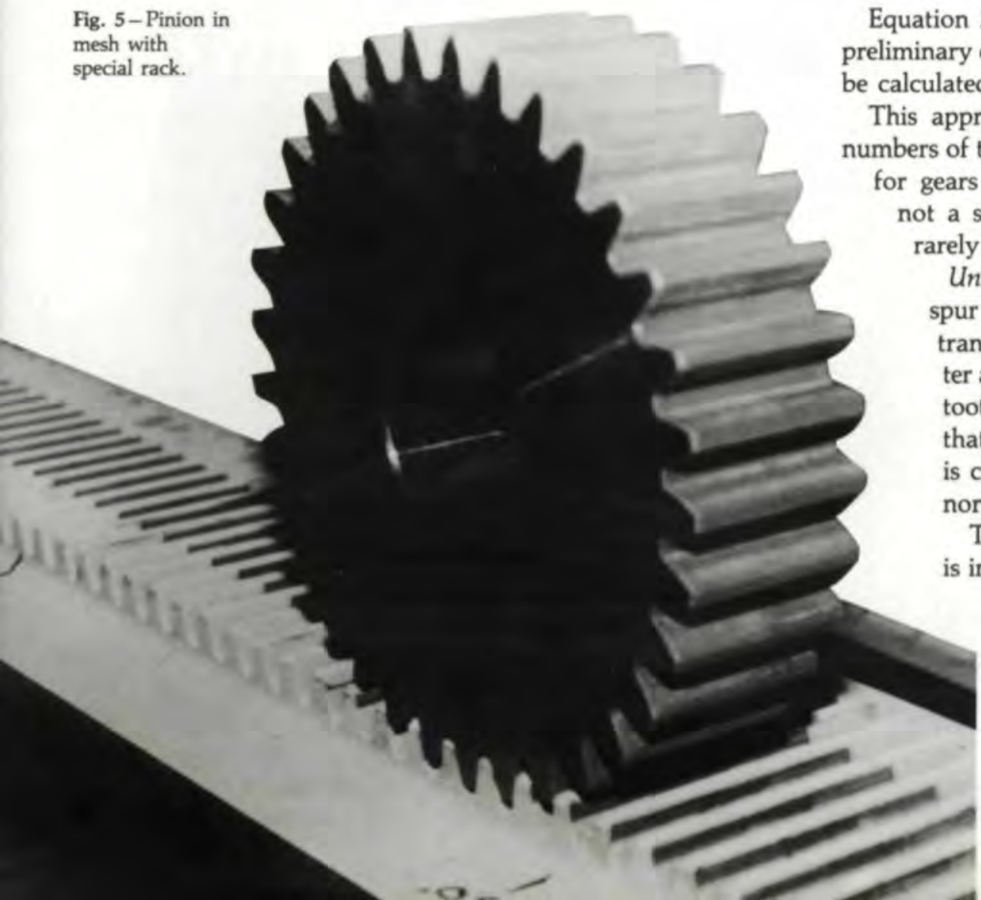

Fig. 5 – Pinion in mesh with special rack.

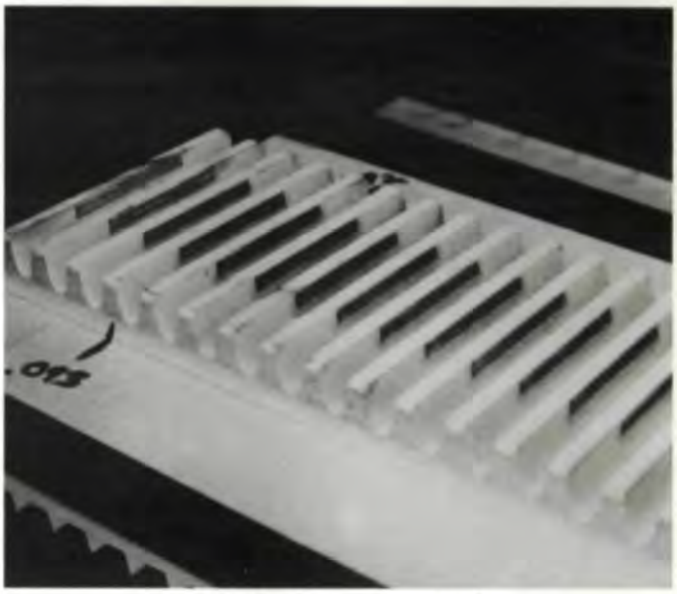

Fig. 6 – Special 8° generated rack.

From Equation 14 the involute function at any diameter where the ratio of tooth thickness to circular pitch is known can be calculated. If we assume that the pressure angle at the limiting outside diameter will be approximately 40°, the ratio of base pitch to circular pitch at the outside diameter will be .776, the cosine of 40°. These assumptions let us derive the following:

$$\text{inv}\phi_{Dmax} = \frac{\pi(t_{bn} - .08p_N)}{N\ p_N} \tag{21}$$

Equation 21 is a good guide to maximum diameter for preliminary design of pinions, but the actual tip land should be calculated before the design is finalized.

This approximation is not useful for gears with large numbers of teeth, since the 40° approximation is unrealistic for gears with more than 40 teeth. This limitation is not a serious one, since the problem is encountered rarely in gears with large numbers of teeth.

Universal Pin Size. Grosser demonstrated that for spur gears, a pin with a diameter equal to half the transverse base pitch will always rest with its center at the diameter where the space width equals the tooth thickness. (See Equation 13). It is easy to show that this is also true for helical gears if the pin size is chosen so that the pin size is equal to half the normal base pitch.

The involute function at that diameter is T, which is independent of the helix angle. The diameter is, of course, a function of D_b, which is inversely proportional to ψ_b. This relationship provides an easy universal way to determine a pin size without tables or long calculation if T is known.

This line of reasoning returns us to the

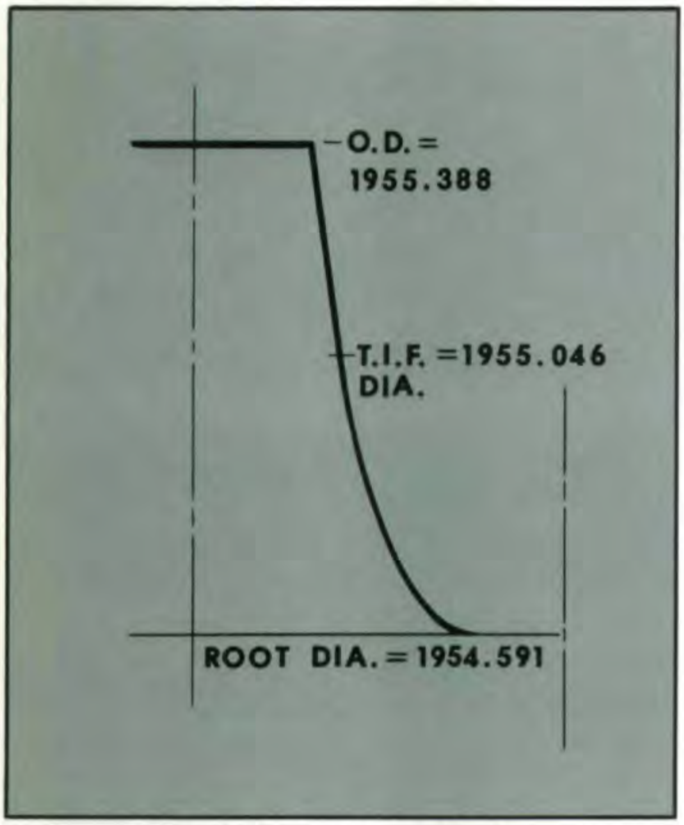

Fig. 7 – Plotted profile of special rack.

concept that a logical relationship should exist between the descriptions of nonstandard helical gears and similar nonstandard spur gears. The T factor does this by giving gears with the same fundamental geometry the same name.

Shaving Cutters. Combining Equation 15 with Equation 12 and eliminating the backlash term, since shaving cutters are in tight mesh,

$$N_1 \text{inv}\phi'_1 + N_2 \text{inv}\phi'_2 = T_1N_1 + T_2N_2 \qquad (22)$$

Also, since the normal operating pressure angle is identical on both parts,

$$\sin\phi'_1 \cos\psi_{b1} = \sin\phi'_2 \cos\psi_{b1} \qquad (23)$$

This pair of equations, which are a rearrangment of those presented by National Broach[9] must be solved by iteration. The solution is beyond the scope of this article, but the equations are presented here to illustrate the value of the T factor in describing a nonstandard gear and simplifying the form of most gear geometry equations.

Conclusions

The equations derived and demonstrated above are not dependent on the T factor. Similar relationships can be derived from the fundamental parameters given at the beginning of this article. Is it really worthwhile to introduce another pet theory into the gear geometry literature? Why not work with t_{bn} and p_N?

At times we need to compare two designs of different pitches to get a sense of how a new design compares to a known set in the field. If we can make the comparison on a nondimensional parametric basis, we can generalize the information and help with future designs too.

The appeal of the x factor system amply demonstrates the need for a comparison factor. The T factor is proposed as a more clearly defined and more useful parameter. By eliminating the assumed cutter definition and the assumed backlash from the parameter, we can compare designs made with nonstandard cutters as easily as we can compare more conventional gears.

Appendix A – Derivations

Symbols

Symbols used are the same as those in the body of the article. The prime symbol (′) denotes values at the operating pitch diameters.

Parallel Axis Gears

Conditions:

- Axes are parallel.
- Transverse operating circular pitches are equal.
- Transverse operating pressure angles are equal.
- Sum of transverse operating tooth thicknesses and transverse operating backlash equals transverse operating circular pitch.

(continued on page 22)

FORMASTER

GRINDING WHEEL PROFILER

EASY TO INSTALL — Because of its small size and weight, the **FORMASTER** does not require major machine modifications and can be installed on nearly any grinder. Installation can usually be accomplished in less than a day.

EASY TO OPERATE — Two axis design simplifies programming and operation. You can choose between four popular controls that feature menu and G-Code programming, graphic simulation, automatic corner rounding, automatic diamond thickness compensation, and more.

IMPROVES ACCURACY

MADE IN U.S.A.

REDUCES WHEEL DRESSING TIME

Patent No. 4,559,919

ACCURATE — To within ± .0001″ of programmed dimension, with repeat accuracy to within .00006″. Extra precision roller bearing ways, pre-loaded roller screws and optical linear encoders, as well as superior design and construction, give the **FORMASTER** the ability to hold inspection gage accuracy.

PRODUCTIVE — No templates or special diamond rolls are needed, so lead times and tooling inventories are reduced. Most forms can be programmed and dressed in, ready to grind in 30 to 45 minutes. Refreshing the form between grinding passes is accomplished in seconds.

VERSATILE — Can be used with single point diamonds or with optional rotary diamond wheel attachment. Nearly any form can be dressed quickly, easily and accurately.

DURABLE — Hard seals are closely fitted and are air purged to totally exclude contamination. Sealed servo motors, automatic lubrication and totally enclosed encoders minimize down time and ensure long service life.

P.O. Box 69
Arden, NC 28704
(704) 684-1002

NORMAC

P.O. Box 207
Northville, MI 48167
(313) 349-2644

CIRCLE A-19 ON READER REPLY CARD

DESCRIBING NONSTANDARD GEARS . . .
(continued from page 20)

Derivation of Equation 5:

$$p' = t'_1 + t'_2 + B'$$

$$p' = D'_1 \left(\frac{t_{b1}}{D_{b1}} - inv\phi'\right) + D'_2 \left(\frac{t_{b2}}{D_{b2}} - inv\phi'\right) + B'$$

$$\frac{p'}{D'_1} = \frac{t_{b1}}{D_{b1}} - inv\phi' + \frac{D'_2}{D'_1}\frac{t_{b2}}{D_{b1}} - \frac{D'_2}{D'_1} inv\phi' + \frac{B'}{D'_1}$$

$$\frac{p'}{D'_1} = \frac{p_b}{D_{b1}}$$

$$\frac{D'_2}{D'_1} = \frac{D_{b2}}{D_{b1}}$$

$$\frac{B'}{D'_1} = \frac{B}{D_{b1}}$$

Note: B' is transverse backlash at D'.
B is transverse backlash in plane of action.

$$p_b = t_{b1} - D_{b1}\, inv\phi' + t_{b2} - D_{b2}\, inv\phi' + B$$

$$inv\phi' (D_{b1} + D_{b2}) = t_{b1} + t_{b2} + B - p_b$$

$$inv\phi' = \frac{t_{b1} + t_{b2} + B - p_b}{D_{b1} + D_{b2}}$$

Crossed Axis Gears

Conditions:

- Axis are in parallel planes.
- Normal operating circular pitches are equal.
- Normal operating pressure angles are equal.
- Sum of normal operating tooth thicknesses plus normal circular backlash equals operating normal circular pitch.

Derivation of Equation 12:

Given: t_{bn1}, t_{bn2}, B_n, N_1, N_2, p_N, p_{x1} and p_{x2}

Note that axial pitches are different for the two gears.

$$p'_{n1} = p'_{n2} = t'_{n1} + t'_{n2} + B_n$$

For each gear:

$$p'_t = \frac{\pi D'}{N} \qquad t'_n = t'_t \cos\phi'$$

$$p'_n = p'_t \cos\psi' \qquad D'\cos\psi' = \frac{N\, p'_n}{\pi}$$

$$\frac{t_{tb}}{D_b} = \frac{\pi\, t_{nb}}{N p_N}$$

$$p'_n = p'_{n1} = p'_{t1}\cos\psi'_1 = \frac{\pi\, D'_1 \cos\psi'_1}{N_1}$$

$$p'_n = D'_1\cos\psi'_1\left(\frac{\pi\, t_{nb1}}{N_1 p_n} - inv\phi'_{t1}\right) + D_2\cos\psi'_2\left(\frac{\pi\, t_{nb2}}{N_2 p_n} - inv\phi'_{t2}\right) + B_n$$

$$p'_n = p'_n\left(\frac{t_{nb1}}{p_N} + \frac{t_{nb2}}{p_N}\right) - \frac{p'_n N_1}{\pi} inv\phi'_{t1} - \frac{p'_n N_2}{\pi} inv\phi'_{t2} + B_n$$

$$1 = \frac{t_{nb1}}{p_N} + \frac{t_{nb2}}{p_N} - \frac{N_1}{\pi} inv\phi'_{t1} - \frac{N_2}{\pi} inv\phi'_{t2} + \frac{B_n}{p'_n}$$

$$\left(\frac{B_n}{p'_n} = \frac{B_N}{p_n}\right)$$

$$N_1 inv\phi'_{t1} + N_2 inv\phi'_{t2} = \frac{\pi}{p_N}(t_{bn1} + t_{bn2} + B_N) - \pi =$$

$$T_1 N_1 + T_2 N_2 + \frac{\pi_{BN}}{p_N} \qquad (22)$$

$$\text{or} \ldots = N_1\left(\frac{t_{b1}}{D_{b1}}\right) + N_2\left(\frac{t_{b2}}{D_{b2}} + \pi\left(\frac{B_N}{p_N}\right) - \pi \qquad (12)$$

Tooth Thickness (See Fig. 8.)

Derivation of Equation 13:

R_1 is the radius where:
"t" = tooth thickness is equal to "s" = tooth space.
ϕ_1 is the pressure angle at that radius.
R_b is the base circle radius.

$$\frac{p_b}{4R_b} + \text{inv}\phi_1 = \frac{t_b}{2R_b}$$

$$\text{inv}\phi_1 = \frac{t_b - \frac{p_b}{2}}{D_b} \quad (13)$$

For any value of t_1:

$$\text{inv}\phi_1 = \frac{t_b}{2R_b} - \frac{p_b}{2R_b}\,\frac{t_1}{p_1}$$

$$\text{inv}\phi_1 = \frac{t_b - p_b t_1/p_1}{D_b} \quad (14)$$

where p_1, ϕ_1 and t_1 are at D_1

Derivation of Equation 21.

If .300″/p_{nd} is a reasonable limit for tip land, t_o:

$$p_{nd} = \frac{\pi}{p} = \frac{\pi \cos\phi_c}{p_N} \text{ and } t_o = \frac{.300\ p_N}{\pi\cos\phi_c}$$

for 14.5°, $t_o = .099p_N$
for 20°, $t_o = .101p_N$
for 25°, $t_o = .105p_N$

Use $.1p_N$ as an approximation.

$$\text{inv}\phi_o = \frac{t_b - p_b(.1p_N)/p_o}{D_b} \quad (14)$$

If we assume that 40° is a good approximation for ϕ_o, $p_o = p_N/\cos 40°$.

$$\text{inv}\phi_{Dmax} = \frac{t_b - p_b(.1p_N.776/p_N)}{p_b}$$

$$\text{inv}\phi_{Dmax} = \frac{t_b - .08p_b}{D_b} \quad (21)$$

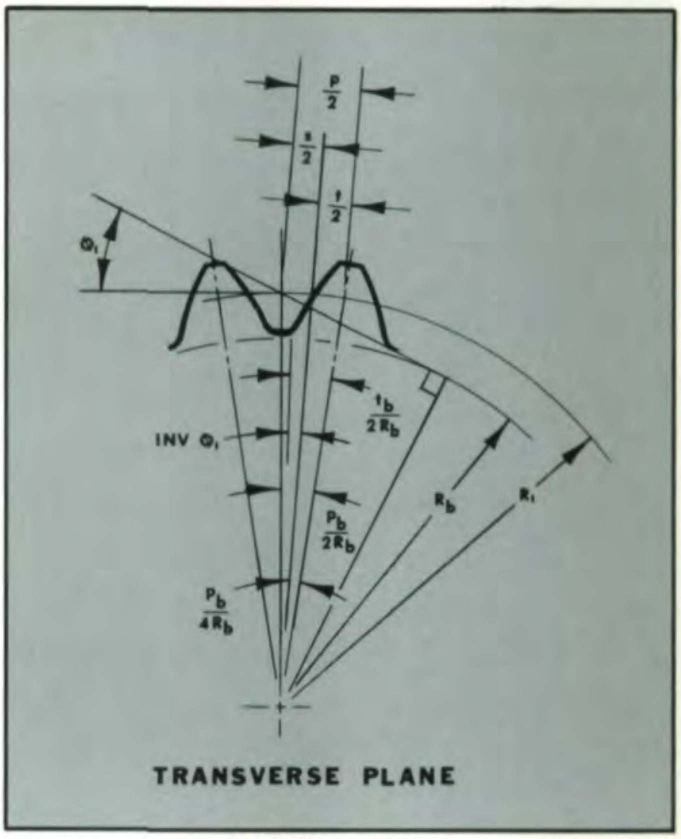

Fig. 8 – Transverse plane.

(continued on page 26)

MIKRON®

CNC GEAR HOBBER

For producing high quality spur and helical gears.

Model A35 with optional gantry type parts handler.

Horizontal Workpiece Clamping
Allows for simplified adaptation of standard parts handling equipment and provides optimum stability when performing both climb and conventional hobbing.

Flexibility and Modularity
Basic unit is designed for quick manual loading *and is expandable to a fully automatic machine* by adding an integrated gantry type parts handling and storage system. Basic 7-axis CNC machine can be expanded to 24-axis to control all types of handling equipment.

Engineering Capabilities
Mikron has extensive CNC experience, having manufactured more than 2,500 precision CNC *machine tools over the past five years.*

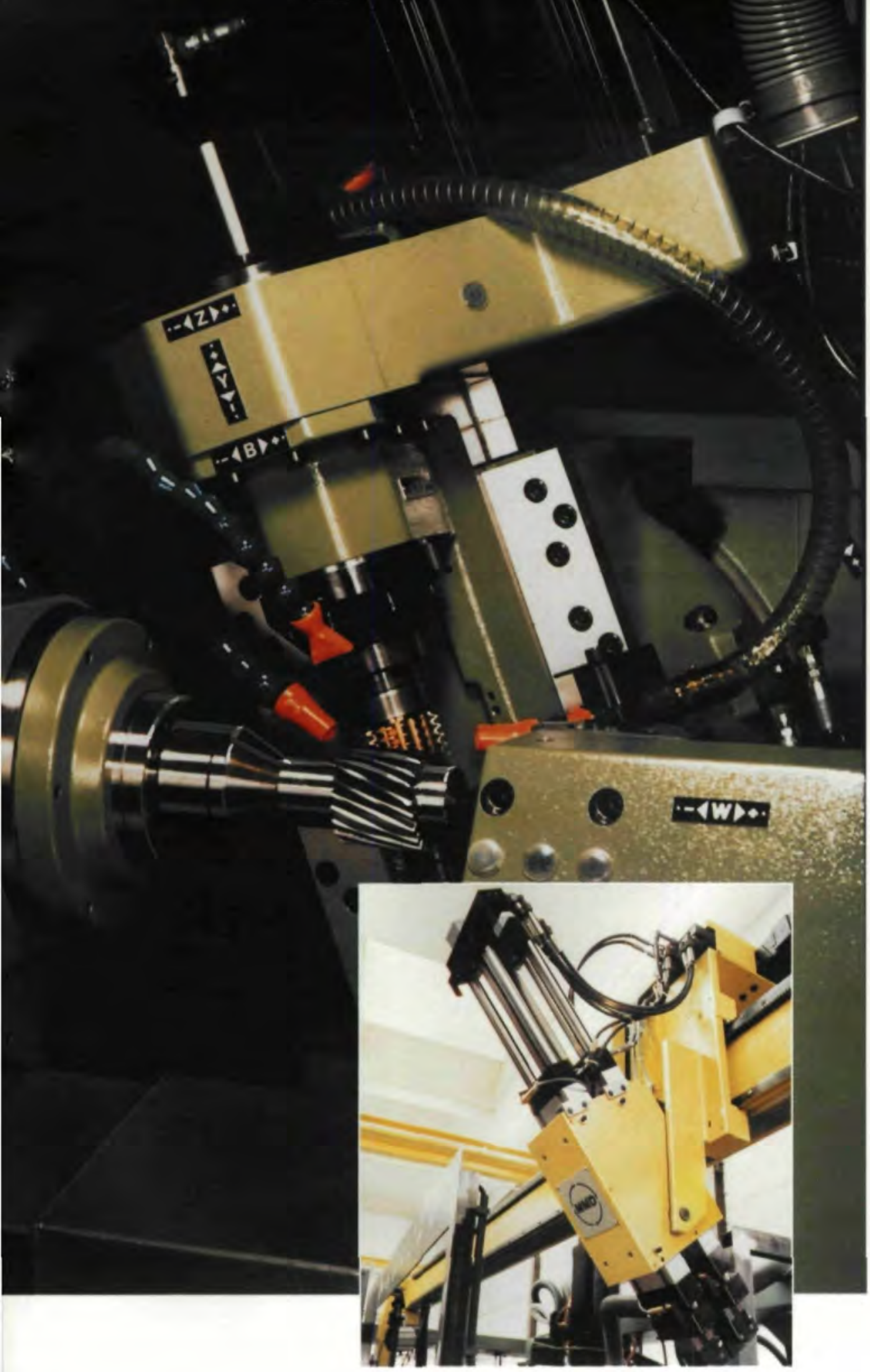

DESCRIBING NONSTANDARD GEARS . . .
(continued from page 23)

Appendix B – Numerical Examples

Description Example:	1	2	2A	3	4	5	6	7
No. Pinion Teeth	23	23	23	20	20	20	33	9999
No. Gear Teeth	35	35	35	35	−71	−71	9999	35
Normal Base Pitch	0.5904	0.5904	0.5904	0.5904	0.9840	0.9840	0.6083	0.5904
Norm. Base Tooth Thk., P	*0.4208*	*0.4536*	*0.4450*	*0.3674*	*0.6120*	*0.5247*	*0.4131*	*36.3831*
Norm. Base Tooth Thk., G	0.4863	0.4536	0.4620	0.4536	0.1460	0.1460	2.0747	0.4536
Axial Pitch	1.5552	1.5552	1.5552	1.5552	–	–	–	1.5552
Addendum Dia., Pinion	5.5580	5.6540	5.6290	4.7730	7.5800	7.3300	7.2500	2186.67
Addendum Dia., Gear	8.2470	8.1510	8.1760	8.1510	−23.2000	−23.2000	1955.4570	8.1510
"T" Pinion	0.029054	0.036632	0.034652	0.019203	0.019156	0.005220	0.017047	0.019204
"T" Gear	0.029050	0.024073	0.025356	0.024073	0.015559	0.015559	0.000914	0.024073
"Phi T" Pinion	0.4320	0.4648	0.4567	0.3787	0.3784	0.2481	0.3645	0.3787
Degrees	24.7544	26.6291	26.1686	21.6969	21.6798	14.2160	20.8835	21.6971
"Phi T" Gear	0.4320	0.4070	0.4138	0.4070	0.3539	0.3539	0.1396	0.4070
Degrees	24.7534	23.3205	23.7088	23.3205	20.2787	20.2787	8.0000	23.3205
Base Helix Angle	0.3894	0.3894	0.3894	0.3894	.0000	.0000	.0000	0.3894
Degrees	22.3122	22.3122	22.3122	22.3122	.0000	.0000	.0000	22.3122
Center Dist. Fixed?	1	1	1	0	0	0	0	0
Center Distance	6.5000	6.5000	6.5000	6.0583	−8.4818	−8.6049	981.1751	1096.96
Normal Backlash	*0.0100*	*0.0100*	*0.0100*	*0.0000*	*0.0000*	*0.0000*	*0.0050*	*0.0000*
Inv. Oper. Press. Angle	0.029951	0.029951	0.029951	0.022302	0.014148	0.019613	0.000970	0.019221
Cos. Oper. Press. Angle	0.906355	0.906355	0.906355	0.922136	0.941665	0.928200	0.989880	0.929112
Operating Press Angle	0.4362	0.4362	0.4362	0.3972	0.3433	0.3813	0.1424	0.3788
Degrees	24.9936	24.9936	24.9936	22.7597	19.6668	21.8441	8.1582	21.7033
Gen. Helix Angle, Pinion	0.4159	0.4159	0.4159	0.4159	.0000	.0000	.0000	0.4159
Degrees	23.8297	23.8297	23.8297	23.8297	.0000	.0000	.0000	23.8297
Gen. Helix Angle, Gear	0.4159	0.4159	0.4159	0.4159	.0000	.0000	.0000	0.4159
Degrees	23.8297	23.8297	23.8297	23.8297	.0000	.0000	.0000	23.8297
Tip Land, Pinion	0.1414	0.1225	0.1277	0.1609	0.1096	0.1624	0.1498	0.1442
Tip Land, Gear	0.1449	0.1574	0.1543	0.1574	0.3453	0.3453	0.2608	0.1574
Whole Depth, Pinion	0.452	0.453	0.453	0.450	0.835	0.837	0.228	0.500
Whole Depth, Gear	0.453	0.453	0.453	0.453	0.671	0.671	0.232	0.453
X FACTORS								
X Pinion (Thickness)	0.3112	0.5507	0.4881	.0000	0.1163	−0.2664	0.7339	−0.0005
X Gear (Thickness)	0.4734	0.2341	0.2958	0.2341	−0.0622	−0.0622	−0.0466	0.2341
X Pinion (Diameter)	*0.3233*	*0.5633*	*0.5008*	*0.0006*	*0.3700*	*−0.0050*	*0.6250*	*0.25*
Backlash Allow. Pinion	0.0019	0.0020	0.0020	0.0001	0.0616	0.0635	−0.0113	0.04
X Gear (Diameter)	0.4866	0.2466	0.3091	0.2466	−0.3000	−0.3000	−0.1180	0.2466
Backlash Allow. Gear	0.0021	0.0020	0.0021	0.0020	−0.0577	−0.0577	−0.0072	0.0020
PINION CUTTER DATA								
Normal DP	5.0000	5.0000	5.0000	5.0000	3.0000	3.0000	5.0000	5.0000
Normal Module (mm)								
Profile Angle	20.0000	20.0000	20.0000	20.0000	20.0000	20.0000	14.500	20.0000
Profile Angle (RAD)	0.3491	0.3491	0.3491	0.3491	0.3491	0.3491	0.2531	0.3491
Circular Pitch	0.6283	0.6283	0.6283	0.6283	1.0472	1.0472	0.6283	0.6283
Cutter Thickness	0.3142	0.3142	0.3142	0.3142	0.5236	0.5236	0.3142	0.3142
Cutter Addendum	0.2500	0.2500	0.2500	0.2500	0.4167	0.4167	0.2500	0.2500

Appendix B — Numerical Examples (continued)

Description Example:	1	2	2A	3	4	5	6	7
GEAR CUTTER DATA								
Normal DP	5.0000	5.0000	5.0000	5.0000	3.0000	3.0000	5.1141	5.0000
Normal Module (mm)								
Profile Angle	20.0000	20.0000	20.0000	20.0000	20.0000	20.0000	8.0000	20.0000
Profile Angle (RAD)	0.3491	0.3491	0.3491	0.3491	0.3491	0.3491	0.1396	0.3491
Circular Pitch	0.6283	0.6283	0.6283	0.6283	1.0472	1.0472	0.6143	0.6283
Cutter Thickness	0.3142	0.3142	0.3142	0.3142	0.5236	0.5236	0.1912	0.3142
Cutter Addendum	0.2500	0.2500	0.2500	0.2500	0.4167	0.4167	0.0500	0.2500
DIAMETERS								
Base Diameter, Pinion	4.6724	4.6724	4.6724	4.0630	6.2643	6.2643	6.3898	2031.28
Base Diameter, Gear	7.1102	7.1102	7.1102	7.1102	−22.2384	−22.2384	1936.1013	7.1102
Generating Dia. Pinion	5.0287	5.0287	5.0287	4.3728	6.6667	6.6667	6.6000	2186.17
Generating Dia. Gear	7.6524	7.6524	7.6524	7.6524	−23.6667	−23.6667	1955.1121	7.6524
Operating Dia. Pinion	5.1552	5.1552	5.1552	4.4060	6.6524	6.7489	6.4551	2186.26
Operating Dia. Gear	7.8448	7.8448	7.8448	7.7106	−23.6160	−23.9586	1955.8950	7.6527
Max. Add. Dia. Pinion	5.6575	5.7196	5.7035	4.9076	7.5661	7.4067	7.3958	2186.86
Max. Add. Dia. Gear	8.3652	8.2973	8.3150	8.2973	ERR	ERR	1956.8395	8.2973
Addendum Dia. Pinion	5.5580	5.6540	5.6290	4.7730	7.5800	7.3300	7.2500	2186.67
Addendum Dia. Gear	8.2470	8.1510	8.1760	8.1510	−23.2000	−23.2000	1955.4570	8.1510
Std. Add. Dia. Pinion	5.4287	5.4287	5.4287	4.7728	7.3333	7.3333	7.0000	2186.57
Std. Add. Dia. Gear	8.0524	8.0524	8.0524	8.0524	−23.0000	−23.0000	1955.5031	8.0524
Root Dia. Pinion	4.6532	4.7490	4.7239	3.8728	5.9109	5.6557	6.7935	2185.670
Root Dia. Gear	7.3417	7.2460	7.2707	7.2460	−24.5415	−24.5415	1954.9939	7.2460
RADIAL CLEARANCE								
Pinion Root Clearance	0.0499	0.0500	0.0500	0.0464	0.1627	0.1673	0.0498	0.0475
Gear Root Clearance	0.0501	0.0500	0.0502	0.0488	−0.0011	0.0009	0.0531	−0.0002
Standard Clearance	0.0500	0.0500	0.0500	0.0500	0.0833	0.0833	0.0500	0.0500
DIMENS. IN TRANSV. PLANE								
Base Pitch	0.6382	0.6382	0.6382	0.6382	0.9840	0.9840	0.6083	0.6382
Operating Circ. Pitch	0.7042	0.7042	0.7042	0.6921	1.0450	1.0601	0.6145	0.6869
Base Tooth Thick., Pin.	0.4549	0.4903	0.4810	0.3971	0.6120	0.5247	0.4131	39.3276
Base Tooth Thick., Gear	0.5257	0.4903	0.4994	0.4903	0.1460	0.1460	2.0747	0.4903
Tooth Thick., Gen. Pin.	0.3930	0.4311	0.4211	0.3434	0.5518	0.4589	0.3901	0.3434
Tooth Thick., Gen. Gear	0.4188	0.3807	0.3905	0.3807	0.5085	0.5085	0.3094	0.3807
Tooth Thick., Std. Pin.	0.3434	0.3434	0.3434	0.3434	0.5236	0.5236	0.3142	0.3434
Tooth Thick., Std. Gear	0.3434	0.3434	0.3434	0.3434	0.5236	0.5236	0.3142	0.3434
Press. Angle, Gen. Pin.	0.3787	0.3787	0.3787	0.3787	0.3492	0.3492	0.2531	0.3787
Degrees	21.6971	21.6971	21.6971	21.6971	20.0070	20.0070	14.5000	21.6971
Press. Angle, Gen. Gear	0.3787	0.3787	0.3787	0.3787	0.3492	0.3492	0.1396	0.3787
Degrees	21.6971	21.6971	21.6971	21.6971	20.0070	20.0070	7.9966	21.6971

(continued on page 48)

KHV Planetary Gearing - Part II

David Yu
MCP Products Corp.
Skokie, IL

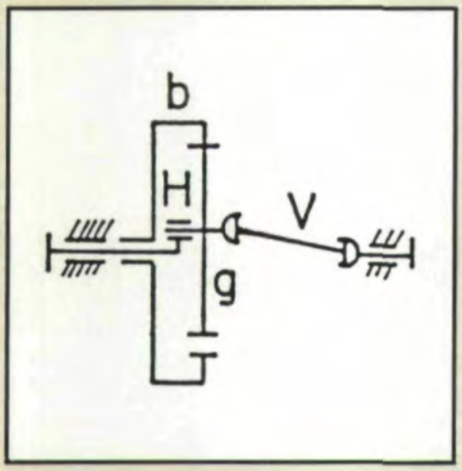

Fig. 1—KHV gearing.

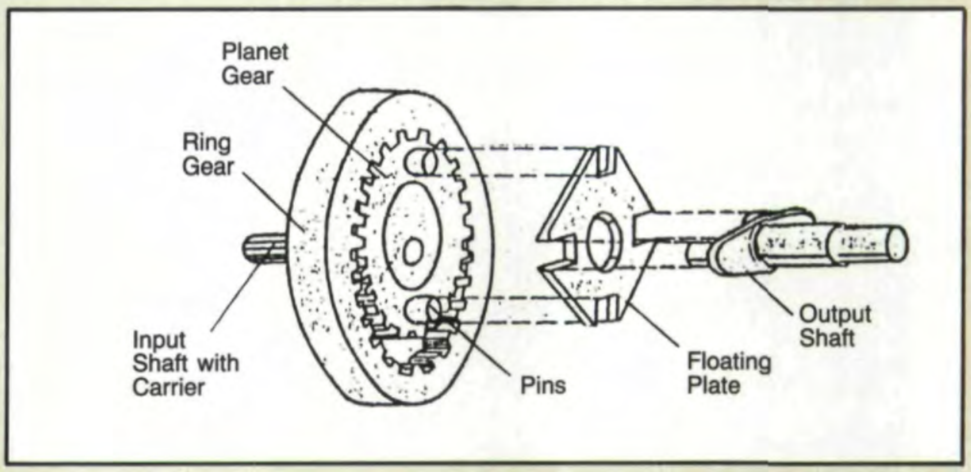

Fig. 2—KHV with floating plate equal velocity mechanism.

Abstract

In Part I of this article, various types of planetary gears were surveyed and the KHV type was recommended as having potential for wider use with medium power transmissions and larger speed ratios. Part II continues the discussion, showing ways to decrease the pressure angle during meshing, improving force distribution and raising efficiency. Having analyzed the calculated data of 400 examples, the author has shown that the efficiency of a KHV does not reduce with the increasing speed ratio and may reach a higher value of 92%. The author's Fortran program for optimizing the parameters is shown.

Introduction

Consisting of only a ring gear b meshing with one or two planets a, a carrier H and an equal velocity mechanism V, a KHV gearing (Fig. 1) is compact in structure, small in size and capable of providing a large speed ratio. For a single stage, its speed ratio can reach up to 200, and its size is approximately 1/4 that of a conventional multi-stage gear box.

If the ring gear b is fixed and the carrier H is the input, the planet must be the output. Through the principle of relative angular velocity, the speed ratio between H and P can be obtained as follows:

$$r_{ha} = \frac{N_h}{N_a} = \frac{-Z_a}{Z_b - Z_a} \qquad (1)$$

Where: r_{ha} is the speed ratio from H to a,
N_h and N_a are angular velocities of H and a respectively,
Z_b and Z_a are numbers of teeth of the ring gear b and the planet a respectively.

For example, if $Z_b = 100$ and $Z_a = 99$, the speed ratio $r_{ha} = -99$.

The equal velocity mechanism is used to transmit the motion and power of the planet to a shaft, the axis of which coincides with the central axis of the gearing. Any coupling that can transmit motion between two parallel shafts, such as, an Oldman coupling or a Hookes joint, (See Fig. 1.) can be used as the equal velocity mechanism V. However, these kinds of coupling are too large and too heavy, which would tend to nullify the advantages of the KHV. Therefore, special designs should be used.

One of them is the floating plate type shown in Fig. 2. There are also other types of equal velocity mechanisms, such

AUTHOR:

DR. DAVID YU *is a gearing specialist for MPC Products Corporation. Since 1982 he has been an Honorary Fellow of the University of Wisconsin at Madison. In the academic arena, he has served as the Deputy Head of the Mechanical Engineering Department, and as Professor of Machine Design at Overseas Chinese University. Professor Yu is the author of numerous articles on gearing. He is a member of CMES, JSME and ASME Gear Research Institute.*

as plate shaft type, zero tooth-difference type, etc.

The KHV planetary driving with involute toothed gears is one of the most promising gearings. With only one internal gear and one pinion, the KHV has many prominent advantages, such as compact structure, light weight, and fewer manufactured machine parts. But the KHV also has shortcomings. Its mechanical efficiency has been considered low. The larger the transmission ratio, the lower the efficiency. Interference is liable to occur, and the calculation of its geometrical dimension is complicated. Therefore, at present, KHV gears can only be used in small power tramsmission. Whether their efficiency can increase and will not drop sharply when speed ratio becomes large are important concerns for the further development of KHV gearing.

In this article the author will present a new concept, which was verified through about 400 examples with various parameters; that is, the efficiency during meshing of KHV gears can reach a higher value and will not decrease with the increasing of speed ratio. This conclusion may open the door for the use of KHV gearing in medium power transmissions and larger speed ratio applications. For example, the pressure angle during meshing adopted by Prof. Muneharu Morozumi is 61.06°, when the tooth difference between internal gear and pinion is one. When the tooth difference is 2, the pressure angle is 46.03°, and when it is 3, the pressure angle is 37.41°.[1] Prof. Bolotvskaya uses a pressure angle of more than 38° when the tooth difference is 3.[2] The larger the pressure angle, the lower the efficiency and the bigger the acting force. But in this paper, the pressure angles are only about 51°, 33°, and 26°, corresponding to tooth difference = 1, 2 and 3, respectively. The efficiency will be 92-98%. These improved results are due to an adequate method for calculating geometrical dimension, accurate efficiency formulae and optimized parameters.

Adequate Method for Calculating Dimension

In calculating external gearing, the methods of determining the geometrical dimension are basically similar. But there are various methods in internal gearing, and different results will be obtained, depending on the method used. In some methods, the formulae for external gearing are directly introduced to internal gearing, with only a change of + or − symbols, and in others, the parameters of the cutter are not taken into account.[3] The internal gearing cut by a pinion type cutter is quite different from the external gearing. The parameters of gear cutters must be taken into account. Otherwise, the calculation seems to be correct, but the obtained dimension cannot provide good meshing qualities, and sometimes interference may occur during practical cutting and assembling. In a worst case scenario, the internal gear cannot be cut, and the involute figure cannot be generated. For example, in calculating KHV gearings, Prof. Muneharu Morozumi does not consider the parameters of cutters. Some data used by him are as follows: the addendum modification coefficient of internal gear is $X_2 = 0.2$ for all KHVs when the tooth difference = 5, and $X_2 = 0$ for all KHVs when the tooth difference = 8.[1] If the gear in the former case is cut by a new standard cutter (GB71-60) with module m=2 millimeters, number of teeth Zc=50, and addendum modification coefficient, Xc=0.578, then the pressure angle during cutting an internal gear with number of teeth $Z_2=65$ is α_{c2}, and

$$\text{inv}\ \alpha_{c2} = (2 \tan 20°)\ (X_2 - Xc)\ /\ (Z_2 - Z_c) + \text{inv}\ 20°$$

$$= 0.72794(0.2 - 0.578)/(65-50) + 0.149 = -0.0034,$$

That is, α_{c2} becomes negative, and the internal gear cannot be cut. In the case of $X_2 = 0$, many standard cutters cannot be used since α_{c2} may be easily smaller than zero.

The method used in this article is based on the following principles.

1. The dedendum circle should be determined by the parameters of the gear cutter because the dedendum circle of a gear or a pinion is generated by the addendum of the gear cutter; that is,

$$R_{f2} = Ac_2 + Rac \quad (2)$$

$$R_{f1} = Ac_1 - Rac \quad (3)$$

or

$$R_{f1} = m\ (0.5Z_1 - f_h + X_1) \quad (4)$$

where R_f = dedendum circle,
Ra = addendum circle,
A = center distance,
X = addendum modification coefficient,
m = module,
f_h = addendum coefficient of hob;

subscripts
1 = pinion,
2 = internal gear,
c = pinion type cutter,
h = hob

Equations 2 and 3 are used for pinion cutter and Equation 4 for the hob.

2. The addendum circle should be determined mainly by meshing qualities, such as ratio contact, necessary clearance, avoiding interference, sliding factor, etc. The calculations of these items are all in connection with addendum circles. Therefore, from one of these items, addendum circles can be preliminarily determined. The simplest item is clearance, which should be chosen. Then

$$Ra_1 = R_{f2} - A_{12} - mC \quad (5)$$

$$Ra_2 = R_{f1} + A_{12} + mC \quad (6)$$

where C=clearance coefficient. For the time being, it is a given value.

From the above obtained addendum circles, contact ratio interference and other required items can be calculated. If they are not satisfied, the value of C should be changed.

Prof. Bolotovskaya's method is a better one. However, she limited C to 0.25 or 0.3.[4] The pressure angle has to become large to avoid trochoidal interference when tooth difference is small. She did not present any paper on tooth differences less than three. If her method was used for tooth differences of one or two, the pressure angle would be very large.

Practically, clearance is not an important quality index, and it is unnecessary to limit clearance within a certain value. A feasible approach can be used to get smaller pressure angle and higher efficiency; that is, using larger clearance, if necessary, to avoid trochoidal interference.

3. The pinion type cutter itself may be taken for a modified gear with addendum modification coefficient Xc. The Xc=0 was used by Prof. Gavlilenko[5] as an average value. Superficially, the parameters of the cutter would be taken into account. Practically, neither the new cutter nor the reground one can always be exactly Xc=0. For example, in a cutter of m=1.5 mm and Zc=68, Xc=0.737 in a new cutter and Xcmin = −0.05 in the reground one. In another cutter of m=4 mm and Zc=9, Xc=0 is for the new one and Xcmin = −0.27 for the old one. Therefore Xc=0 is not the average value; moreover, the average value itself cannot be used in all cases. Otherwise interference may occur in some particular conditions,[3] because each time the cutter is sharpened X_c and other parameters will change. The reasonable method adopted by the author is using the parameters of a new cutter to calculate geometrical dimensions and reexamining the obtained data through the limited parameters of an old one just before it is worn out. The details can be seen in Reference 3.

Accurate Efficiency Formulae

The mechanical efficiency during meshing is an important quality index of planetary gearing. The following formula is often used to calculate efficiency, though there is little difference among various literatures. (See References 6-8.)

$$\eta_{bv} = \eta \,/\, [\eta + (1 - \eta)\,(1 + Z_1/Zd)] \qquad (7)$$

where η_{bv} — efficiency during meshing of a KHV gearing with carrier H taken as a driver, and equal velocity mechanism V as a follower;

η — efficiency of the reference mechanism with the carrier assumed to be stationary;

Zd — tooth difference; i.e., $Z_2 - Z_1$.

The speed ratio is $-Z_1/Zd$, and from Equation 7, it is obvious that when η does not change, η_{bv} will decrease with the increasing of Z_1/Zd or the absolute value of speed ratio. If η is treated in a simple way such as $\eta = 0.98$, it may easily be chosen from a handbook. Then obtain $\eta_{bv} = 0.83$ when $Z_1/Zd = 9$, and $\eta_{bv} = 0.33$ when $Z_1/Zd = 99$. Perhaps this may be the reason why the efficiency of KHV gearing will drop sharply with the increasing speed ratio, and KHV cannot be used in medium power transmissions with larger speed ratios.

However, η is not a constant and will change with speed ratio or number of teeth. Besides, η_{bv} is very sensitive to η. For example, when $Z_1/Zd = 63$, if $\eta = 0.999$, then $\eta_{bv} = 0.9398$; if $\eta = 0.99$, then $\eta_{bv} = 0.607$; and if $\eta = 0.98$, then $\eta_{bv} = 0.43$. Therefore, the accuracy of η is an important factor. Inaccurate formulae may result in inefficiency and even lead to some wrong conclusions.

The formula recommended by Prof. Kudlyavtzev is a rough one in which the contact ratio is taken as a constant.[6] In many other formulae, η only varies with contact ratio E.[7] Practically, η not only depends on E, but also changes with position of pitch point. In conventional gearing or in some other planetary gearings, the pitch point is within the length of contact, so that the difference among various efficiency formulae will not be large, though some formulae are approximate ones. But in KHV gearings, owing to larger pressure angle, pitch point is often out of contact region, sometimes far from it. If the position of pitch point is not taken into account, errors will arise. A more accurate efficiency formula is used in this paper, in which the position has been considered, that is,

$$\eta = 1 - (3.14159/2)\,\mu Ke\,(Z_2 - Z_1) \,/\, (Z_2 Z_1) \qquad (8)$$

Where μ is coefficient of friction, Ke is a coefficient that is determined by the position of pitch point and contact ratio. Various formulae for calculating Ke are listed in Reference 7.

Optimizing Programming

The procedure for calculating the geometrical dimension of KHV gearing is very complicated. Even using a calculator, it may take four to eight hours to solve one problem, so that it is preferable to design a program for general use and to calculate with a computer. Though arduous manual calculating work can be avoided this way, if a program is only a formulae translation, the obtained result may not be a good one. Only after optimizing techniques are used does the program become really useful.

The discussed problem is a nonlinear constrained program in which there are many transcendental functions and some non-unimodal functions. Therefore it is difficult to use the optimizing methods in which derivatives have to be evaluated, and it is appropriate to use direct search techniques.

There are various methods for direct search, such as the Powell method, the Hooke-Jeeve method, etc., that are effective for mathematical examples, especially for quadratic functions. But they may not be successful if they are directly used in a practical engineering problem, such as KHV gearing.

These methods are designed for unconstrained problems, but ours is a constrained one. As introduced in many books, the penalty function can be used to convert a constrained problem into an unconstrained one. The Powell method with penalty function has been tried, but the result is not a good one, since it is not easy to choose a suitable penalty factor, and the conjugate direction, being deduced from quadratic function, is difficult to form in our problem with many transcendental functions. Three other methods have been also tried by the author, and the results are different from one another.

In consideration of the particular features of KHV gearing, a better method has been chosen as follows:

1. There are many variables in the design of KHV gearing. In order to simplify calculation, the master program has been designed with an array of three dimensions of module, number of teeth and the parameters of cutter. But during the optimizing procedure, three independent variables are used. They are clearance coefficient C, addendum modification coefficient of pinion X_1 and the center distance between pinion and gear, A_{12}, i.e., A.

The objective function is for getting the maximum efficiency. The constraints are Gs > 0 to avoid interference, and

E > 1 to assure the continuity of meshing. Gs > 0.02 is used to consider the errors in machining and assembling. Although Yastlebov verified that E might be smaller than 1 in internal gearing,[9] and in Shanghai, China, there are KHV gearing reducers with E = 0.85 that have normally run for over 10 years. E > 1 is used in our design.

In order to be convenient for calculation, a lot of subroutines are used. The subroutine QR is designed for solving involute functions. The subroutine AB is applied to select a value of angle near the solution within an interval of one degree, so that the angle of a given involute function can be evaluated rapidly. The subroutine AX is used to calculate center distance and addendum modification coefficient. The subroutine GE is designed for computing the constraints, and the subroutine EF is used to calculate efficiency.

2. Without using the penalty function, a modification of the Hooke-Jeeve method has been designed so that it can be available for a constrained problem, such as the one that follows.

From an initial base point within the feasible region, start the search for optimum efficiency with three dimensional exploration. If at the test point, the efficiency is not improving or the constraints cannot be satisfied, the exploring direction should be changed. If the local exploration fails in all six directions (including positive and negative), the searching step length should be reduced, and a new local search conducted. If the local search is successful in one or more directions, start a pattern search with an accelerated step. When the search fails to find a better point in all directions and the step length is smaller than the specified value, the iteration should stop, and an optimum or a result near the optimum will be obtained.

3. In order to obtain a higher efficiency and a smaller pressure angle, the iteration begins from a small pressure angle, so that the starting point formed by the input data is out of the feasible region. The modified Hooke-Jeeve method can only be used within a feasible region; therefore, how to find an initial point within this region is important, and the position of this point should be carefully chosen. Otherwise, the final result will not be a good one.

During the procedure to find the initial point within a feasible region, if A, X_1 and C are treated with the same importance, as in a general mathematical problem of three independent variables, the initial point will be bad, and the final result may be far from the real optimum or the speed of convergence may be very slow. If only A changes to get the initial point, the final result will be improved, but still will not be a good one. Since in this practical problem, A is more influential than X_1 or C on objective functions and constraints, a better method has been adopted; that is, X_1 and C simultaneously change with the accelerated step. If the tested point does not improve in approaching the feasible region, increase A by a small step, then try X_1 and C again. Thus, an ideal initial point within the feasible region can be quickly found.

4. The process of this optimizing method is illustrated in Fig. 3, and the flow chart is given in Fig. 4.

Fortran language is used in the program. Different modules, number of teeth and parameters of cutters are input in groups, so that each time the program can calculate at least 100 problems with 2,800 useful data output.

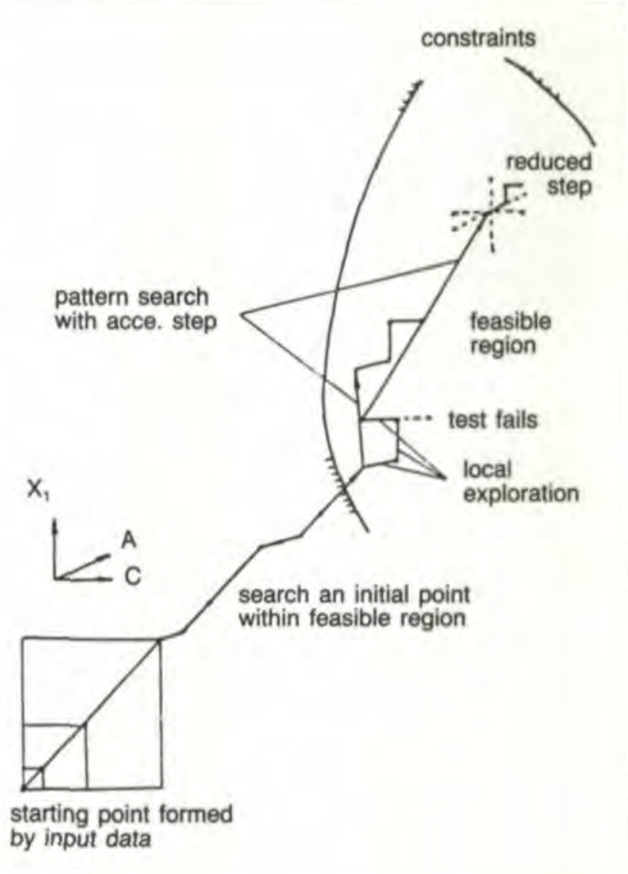

Fig. 3 – The process of the optimizing method.

Conclusion

The author has used this optimizing program to calculate 400 KHV gearings with various different parameters and 11,200 useful data have obtained. Having analyzed the results, we can draw some new conclusions.

1. The mechanical efficiency of the KHV gearing should not be considered low. It can reach a higher value if adequate formulae and optimizing techniques have been used. Some data are listed in Table 1 for illustration, where the coefficient of friction is taken as 0.1.

From Table 1, we can observe that the efficiency does not drop sharply with the increasing of speed ratio. It will be a little larger when tooth difference ($Z_d - Z_2 - Z_1$) increases. However, for a given speed ratio, the size of KHV gearing will become large if tooth difference increases; therefore, tooth difference − 1 should be preferably used in KHV gearing.

2. The pressure angle during meshing is smaller than those presented in other literatures. For comparison, some data are given in Table 2.

Though more experiments should be made to verify the theoretical efficiency obtained from this optimizing program, the calculated 400 KHV gearings all satisfy the constraints and requirements. Therefore, not only the program in this article can be used practically, but also it is certain that, owing to smaller pressure angle, the efficiency and force distribu-

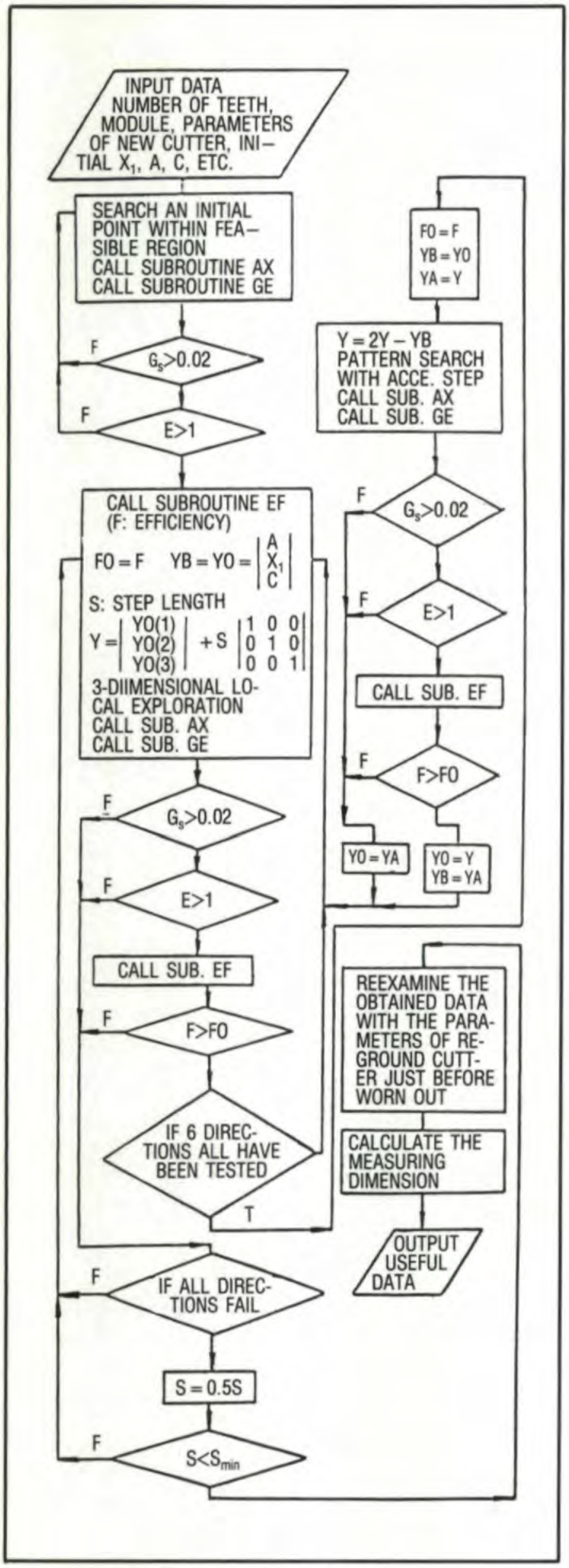

Fig. 4—The flow chart of the program.

Table 1 Some obtained data.

m	Z_d	Z_1	$\frac{-Z_1}{Z_2-Z_1}$	Zc	Xc	Xcmin	α°	$\eta_{nv\%}$
5	1	80	−80	20	0.105	−0.19	51.64	92.22
4	1	100	−100	19	0.105	−0.12	51.21	92.30
3	1	150	−150	34	0.337	−0.15	50.59	92.39
2	1	200	−200	38	0.420	−0.17	50.90	92.23
2	1	250	−250	50	0.578	−0.10	50.59	92.34
1.5	1	300	−300	50	0.503	−0.29	50.16	92.34
1.5	1	360	−360	18	0.103	−0.44	50.16	92.46
5	2	100	−50	20	0.105	−0.19	33.96	97.37
4	2	160	−80	25	0.168	−0.19	33.64	97.34
2	2	200	−100	50	0.578	−0.10	33.74	97.33
1.5	2	320	−160	50	0.503	−0.29	33.48	97.26
3	3	120	−40	25	0.167	−0.13	25.88	99.13
2	3	240	−80	50	0.578	−0.10	25.56	99.06
1.5	3	300	−100	50	0.503	−0.29	25.63	99.01

Table 2 Data for comparison.

David Yu						Muneharu Morozumi		Bolotovskaya		
Z_d	Z_1	m	Zc	Xc	α°	Z_1	α°	Z_1	Zc	α°
1	60	5	25	0.132	51.99	60	61.06			
1	60	4	19	0.105	52.03	60	61.06			
1	80	3	34	0.337	51.52	80	61.06			
1	80	2	50	0.578	51.52	80	61.06			
1	80	1.5	18	0.103	51.41	80	61.06			
2	60	5	20	0.105	34.34	60	46.03			
2	60	3	25	0.167	34.36	60	46.03			
2	80	2	38	0.420	34.11	80	46.03			
2	80	2	50	0.578	34.30	80	46.03			
3	60	4	25	0.168	26.22	60	37.41			
3	60	1.5	18	0.103	26.13	60	37.41			
3	80	3	25	0.167	26.01	80	37.41			
3	80	1.5	18	0.103	26.13	80	37.41			
3	96	4	25	0.168	25.94			97	50	>38
3	96	2	50	0.578	25.94			97	50	>38
3	96	1.5	50	0.503	25.88			97	50	>38

tion are better than those in other designs.

3. After comparision and analysis, an important conclusion can be drawn; that is, the KHV gearing can enter into a wider usage with medium power transmission, larger speed ratio and higher efficiency. In addition to its compact structure, light weight and other advantages, the KHV gearing may become one of the most promising gearings in mechanical transmission.

(continued on page 48)

THE USE OF BOUNDARY ELEMENTS . . .
(continued from page 9)

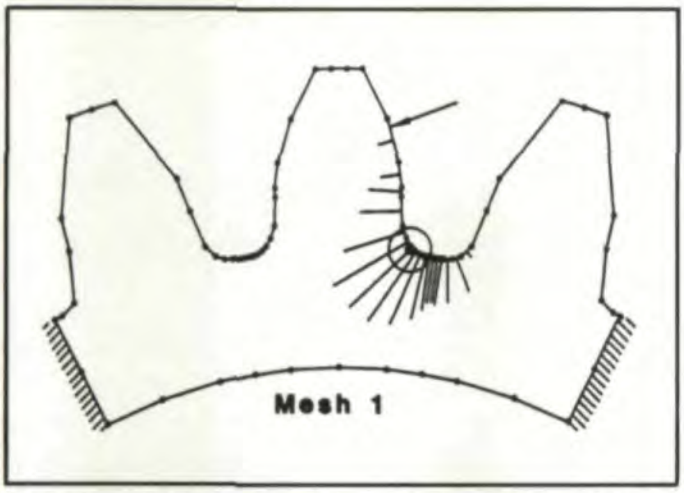

Fig. 3 – Stress distribution along the boundary for a thick rimmed external gear supported at the ends.

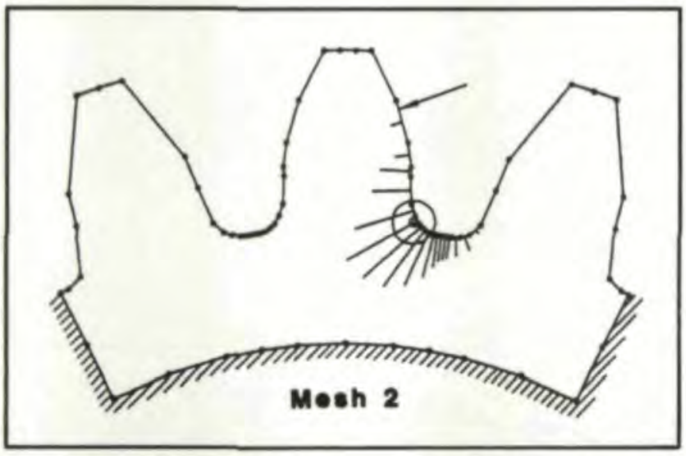

Fig. 4 – Stress distribution along the boundary for a thick rimmed external gear supported along the inner bore.

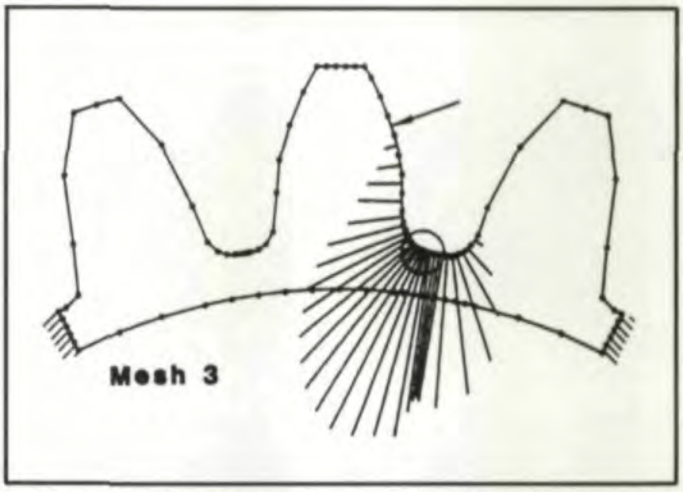

Fig. 5 – Stress distribution along the boundary for a thin rimmed external gear supported at the ends.

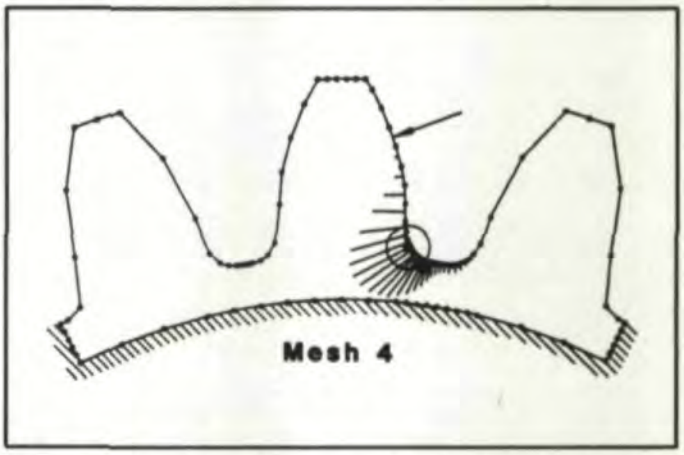

Fig. 6 – Stress distribution along the boundary for a thin rimmed external gear supported along the inner bore.

of the critical stress point did not change, and the J factor was found to increase from 0.335 to 0.343 just by changing the boundary conditions. Mesh 3 (Fig. 5) shows a thin rimmed gear whose rim is unsupported, and Mesh 4 (Fig. 6) shows the same thin rimmed gear with a fixed rim. The boundary condition effect on the J factor is much greater for the thin rimmed case, and the stresses increase when the constraints for the thin rimmed case are removed. The location of the critical point also changes. A computer analysis using the AGMA 218.01 standard gave a value of 0.3019 for the J factor for cases 1 through 4, and the graphs in the AGMA standard give a J factor of about 0.32. Finite element models were also created and run on ANSYS for cases 1 through 4. Fig. 10 shows the finite element model for case 4, and Fig. 11 shows the contour plot of the maximum principal stress for this run. The J factors from the finite element runs are also tabulated in Table 1. The finite element models show stresses that are consistently 10% higher than those obtained by the boundary element models. This may be due to the different techniques used by the two methods in extrapolating the stresses to the surface and needs further investigation. Table 3 shows J factors obtained for gear teeth with the same profile and roots as in cases 1 through 4, as the inner radius is varied from 0.5 to 0.8, with the rim supported only at its edges.

Meshes 5 and 6 (Figs. 7 & 8) show that this approach can also be used with internal gears, and Mesh 7 (Fig. 9) shows how this method can be used with gears with a small number of teeth when undercutting takes place. Plane stress conditions were assumed for these cases, but plane strain conditions could have been used. The decision as to which is more applicable would have to be made by the user.

Summary and Future Research

The boundary element methodology has several advantages over using the standardized gear rating schemes. It can take into account different boundary conditions, account for plane stress or plane strain conditions, determine the actual critical point and include the effects of support conditions and rim thickness. Furthermore, the method can handle internal gears and can also compute displacements. Since the complete multi-axial state of stress at any point is available, any failure theory can be used to identify the critical point and to compute the geometry factor.

The method does, however, have limitations. The state of stress in gear teeth is almost always three-dimensional, and

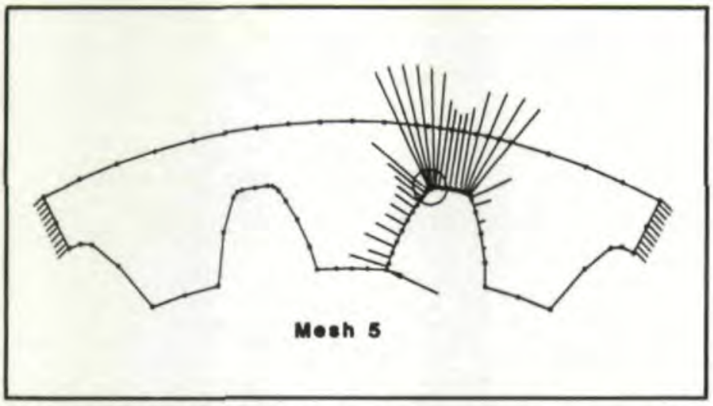

Fig. 7 – Stress distribution along the boundary for an internal gear supported at the ends.

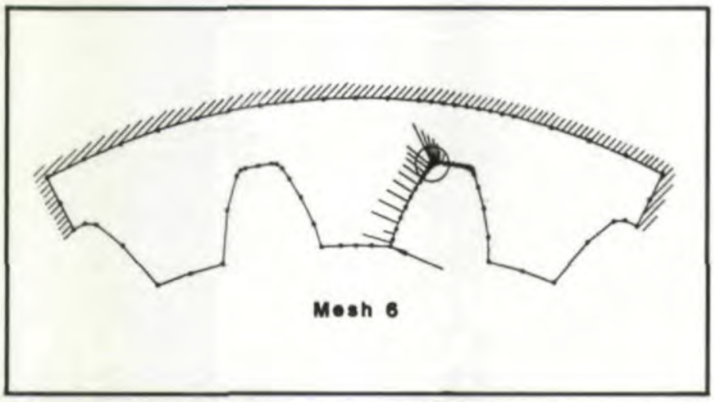

Fig. 8 – Stress distribution along the boundary for an internal gear supported along the outer radius.

Table 3. Variation of the geometry factor with the rim thickness

Inner radius (inches)	Ratio of rim thickness to whole tooth depth	Geometry Factor J
0.50	1.5	0.334
0.70	0.67	0.334
0.75	0.46	0.291
0.80	0.25	0.159

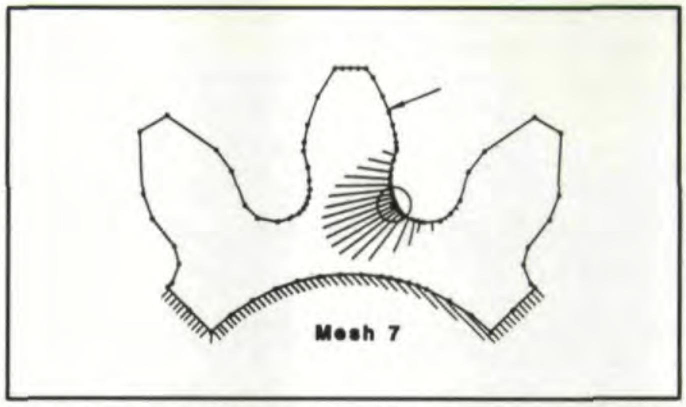

Fig. 9 – Stress distribution along the boundary for an external gear with 12 teeth supported along the inner bore.

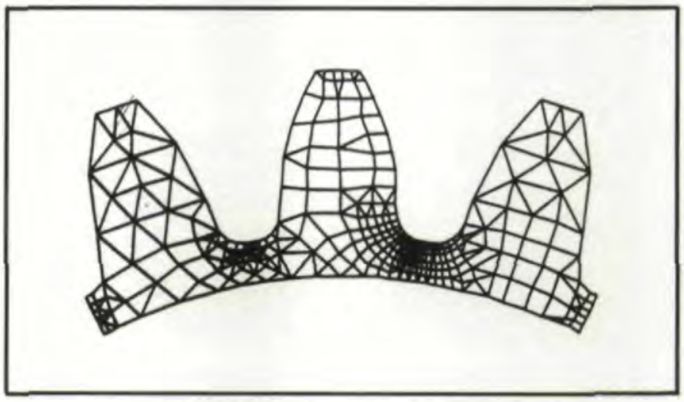

Fig. 10 – Finite element model for case 4.

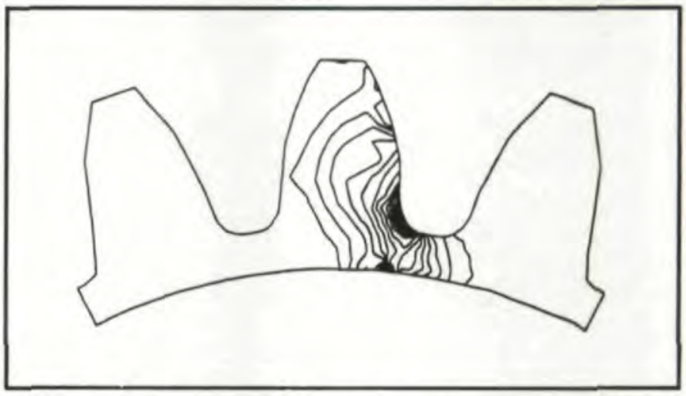

Fig. 11 – Contour plot of maximum principal stress in the finite element model of case 4.

for a complete study, this method cannot replace full fledged three-dimensional finite element analysis, but only supplement it. The boundary element method does not allow stress computations on the boundary, but this limitation can be overcome by computing the stresses at two points near the boundary and extrapolating the values to the boundary. The time required to compute the system matrices varies as the square of the number of nodes. Thus, the efficiency of the method decreases as models get large. Also, unlike the finite element method, the matrices are not banded or symmetric. However, meshes with 100 to 120 nodes serve well enough, and these limitations do not cause any serious problems.

Since only preliminary results are presented here, a considerable amount of case history experience is needed in order to assess the potential of this method more accurately. In particular, there should be some corroboration between J factors computed by the boundary element method and those computed by the AGMA method. The following studies are anticipated in the next year to provide further verification of this method for the evaluation of geometry factors:

- Comparison of boundary element results with current AGMA analysis and with finite element analysis for a broad spectrum of gear and hob geometries. Computation time comparisons with finite element methods will also be made.
- Comparison of boundary element results with computational and experimental results in the literature for thin rimmed gears and internal gears.
- Determine the feasibility of using personal computers for

the geometry factor calculation using boundary elements.

- Enhance the program to take care of the roller boundary conditions and to allow models to incorporate a number of teeth greater than three.

Appendix

Boundary Element Method Equations

Boundary element methods use approximating functions that satisfy the governing elasticity equations within the outer periphery of the body being analyzed, but not the boundary conditions. These functions are called the fundamental solutions.

Figs. 12 & 13 show a typical body which is to be analyzed. The elasticity equations which govern the analysis have been presented here in tensor notation for the sake of conciseness.

For every point in the body of interest to be in a state of equilibrium, the stress field must satisfy the following equilibrium equation:

$$\text{equilibrium: } \sigma_{ij,j} = 0 \text{ in } \Omega$$

Here i and j vary from 1 to 2 for a two-dimensional analysis and Ω is the interior of the body.

The surface loads or the tractions applied to the body are related to the stresses as

$$\text{traction: } \sigma_{ij}n_j = p_i \text{ (prescribed on } \Gamma_2)$$

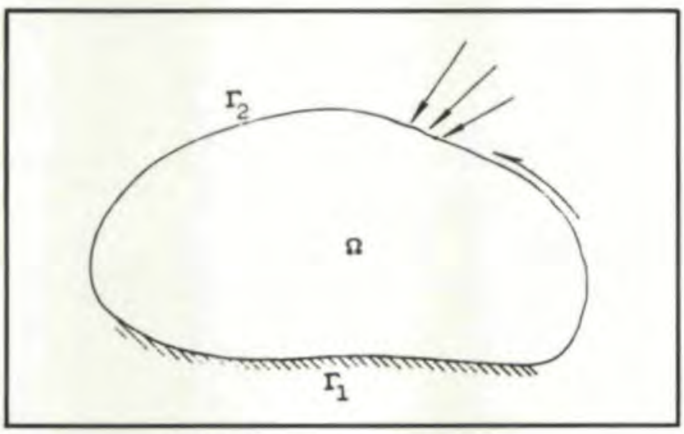

Fig. 12 – Body under consideration.

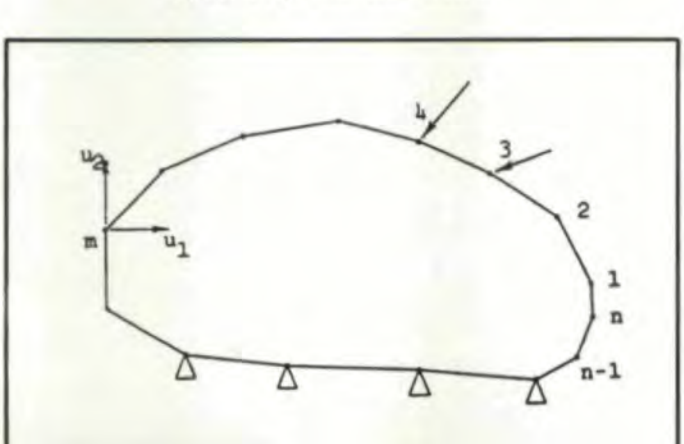

Fig. 13 – Boundary element discretization.

These tractions are prescribed on part of the body's surface Γ_2. On the rest of the surface of the body, the displacements u_i have to be prescribed. σ_{ij} is the stress tensor field and the u_i is the displacement vector field. The starting point for both the boundary element method and the finite element method is an integrated form of the equilibrium equation:

$$\text{for all } u_i^*: \int_\Omega u_i^* \sigma_{ij,j} d\Omega = 0$$

where u_i^* is an arbitrary weighting function. The choice of this weighting function is one of the differences between the boundary and finite element method. In the finite element method, these functions are chosen to be the same as the shape functions, whereas, in the boundary element method, the fundamental solutions are used.

Integrating by parts, (integration by parts in two and three dimensions is carried out using Green's identity) we get:

$$\int_\Gamma u_i^* \sigma_{ij} n_j d\Gamma - \int_\Omega u_{i,j}^* \sigma_{ij} d\Omega = 0$$

But it can be shown that

$$u_{i,j}^* \sigma_{ij} = \sigma_{ij}^* \epsilon_{ij}$$

Therefore, the integral becomes:

$$\int_\Gamma u_i^* \sigma_{ij} n_j d\Gamma - \int_\Omega \sigma_{ij}^* \epsilon_{ij} d\Omega = 0$$

or,

$$\int_\Gamma u_i^* p_i d\Gamma - \int_\Omega \sigma_{ij}^* \epsilon_{ij} d\Omega = 0$$

The above set of equations is characteristic of most finite element developments. However, the boundary element method carries out integration by parts once more:

$$\int_\Gamma u_i^* \sigma_{ij} n_j d\Gamma - \int_\Omega \sigma_{ij}^* \epsilon_{ij} d\Omega = 0$$

As before,

$$\int_\Gamma u_i^* \sigma_{ij} n_j d\Gamma - \int_\Omega \sigma_{ij}^* u_{i,j} d\Omega = 0$$

and using Green's identity to integrate by parts once more, for all u_i^*,

$$\int_\Gamma u_i^* \sigma_{ij} n_j d\Gamma - \int_\Gamma u_i \sigma_{ij}^* n_j d\Gamma + \int_\Omega u_i \sigma_{ij,j}^* d\Omega = 0$$

If we choose the field u_i^* to be the response to a unit concentrated load at point P in the 'k' direction, (Such a field is called a fundamental solution of the equilibrium equation.) then:

$$\sigma_{ij,j}^* + \delta_{ik} \Delta(P) = 0$$

Where δ_{ik} is the Kronecker delta and $\Delta(P)$ is the Dirac delta function.

Hence,

$$\int_\Omega u_i\sigma^*_{ij,j}d\Omega = -\int_\Omega u_i\delta_{ik}\,\Delta(P)\,d\Omega = -c_P u_k(P) \quad (A.1)$$

where

$c_P = 0$ if P lies outside
$c_P = 1$ if P lies inside
$c_P = 0.5$ if P lies on a smooth boundary

In the general case, c_P has to be determined by integration.

We then have:

$$\int_\Gamma u_i\bar{\sigma}_{ij}n_j d\Gamma - \int_\Gamma u_i\sigma^*_{ij}n_j d\Gamma - c_P u_k(P) = 0$$

but $\sigma_{ij}n_j$ = traction vector = p_i

$$\int_\Gamma u_i^* p_i d\Gamma - \int_\Gamma u_i p_i^* d\Gamma - c_P u_k(P) = 0$$

To make this equation discrete, let $u_i = \psi_m u_{mi}$ and $p_i = \psi_m p_{mi}$, where ψ_m are the shape functions defined along the boundary of the body only. We do not need to interpolate u_i and p_i inside the body because the above integral is to be evaluated only on the boundary.

The quantities u_{mi} and p_{mi} are the nodal values of the displacements and the tractions, respectively. At any given node, either u_{mi} or p_{mi} is known and the other value is unknown.

For every source point P and every direction k, we can make the above integral equation discrete to get one linear equation relating the p_{mi} and the u_{mi}. A new point P is then moved from one nodal point to the next and as many equations are generated as there are unknowns. This gives a system of linear equations:

$$[\bar{H} - C]\,u = [G]\,p$$

i.e.

$$[\bar{H} + C]\,u = [G]\,p$$

The matrix [C] contains all of the c_P coefficients. Instead of evaluating them by integrating, an easier way to determine them is by applying rigid body displacements and zero tractions in the above matrix equation.

The system of equations becomes:

$$[H]\,u = [G]\,p$$

which is then solved to determine the unknown tractions and displacements.

Once all of the nodal displacements and tractions are known, Equation (A.1) can be used to determine the displacement of any interior point P. This displacement can then be differentiated to obtain the strains and hence the stresses in the interior of the body.

References

1. AMERICAN GEAR MANUFACTURERS ASSOCIATION. *AGMA Standard For Rating the Pitting Resistance and Bending Strength of Spur and Helical Involute Gear Teeth.* AGMA 218.01, 1982.
2. S. K. WADHWA. "Analytical Determination of Geometry Factor for Shaped Spur Gears." ASME Paper 68-MECH-53, 1968.
3. R. G. MITCHINER. "The Determination of the Lewis Form Factor and the AGMA Geometry Factor J for External Spur Gear Teeth." ASME Paper 80-DET-59, 1980.
4. R. ERRICHELLO. "An Efficient Algorithm for Obtaining the Gear Strength Geometry Factor on a Programmable Calculator." AGMA Paper P139.03, 1981.
5. R. ERRICHELLO. "An Efficient Algorithm for Obtaining the Gear Strength Geometry Factor for Shaper Cut Gears." AGMA Paper P139.05, 1983.
6. R. J. DAVEY, R.T. WHEWAY. "An Exact Mathematical Solution for the Dimensions of the Lewis Equal Strength Parabola." ASME Paper No. 84-DET-183, 1984.
7. RAYMOND J. DRAGO. "Limitations of Current Tooth Root Stress Analysis." AGMA Paper No. 220.20, 1976.
8. RAYMOND J. DRAGO, GARY A. PIZZIGATI. "Some Progress in the Accurate Evaluation of Tooth Root and Fillet Stresses in Lightweight, Thin-Rimmed Gears." AGMA Paper 229.21, 1980.
9. TOSHIYUKI SUZUKI, TAE-HYONG CHONG, TOSHIO AIDA, HIROSHIGE FUJIO, AIZOH KUBO. "Tooth Fillet Stresses of Gear with Thin Rim." *Bulletin of the JSME* Vol. 25, No. 204. June, 1982, 1022-1029.
10. TAE-HYONG CHONG, A. KUBO. "Simple Stress Formulae for a Thin Rimmed Spur Gear. Part 1: Derivation of Approximation Formulae for Tooth Fillet and Root Stresses," ASME Paper No. 84-DET-62, 1984.
11. JARMO ELORANTA, ERIK SANDBERG. "Stress, Deflection and Load Distribution in Thin Rimmed Internal Gears." Second World Gear Congress, Paris, France, March 3-5, 1986. Manufacturing and Checking, 1986.
12. G. CASTELLANI, V. P. CASTELLI. "Rating Gear Teeth," ASME Paper No. 80-C2/DET-88, 1980.
13. TAE-HYONG CHONG, TOSHIYUKI SUZUKI, TOSHIO AIDA, HIROSHIGE FUJIO, AIZOH KUBO. "Tooth Fillet Stresses of Gear with Thin Rim." *Bulletin of the JSME.* Vol. 26, No. 214. April, 1983, 633-640.
14. TAE-HYONG CHONG, TOSHIYUKI SUZUKI, AIZOH KUBO, HIROSHIGE FUJIO. "Tooth Fillet Stresses of Gear with Thin Rim." *Bulletin of the JSME.* Vol. 26, No. 220. October, 1983, 1799-1806.
15. TAKESHI ISHIDA, TERUAKI HIDAKA, HIDEHARU TAKIZAWA. "Bending Stress Analysis of the Idle Gear with Thin Rim." *Bulletin of the JSME.* Vol. 28, No. 241. October, 1985. 2422-2428.
16. TAKESHI ISHIDA, TERUAKI HIDAKA, HIDEHARU TAKIZAWA. "Bending Stress Analysis of Idle Gear with Thin Rim." *Bulletin of the JSME.* Vol. 28, No. 244. July, 1985, 1505-1511.
17. RAYMOND J. DRAGO, RONALD V. LUTTHANS. "An Experimental Investigation of the Combined Effects of Rim Thickness and Pitch Diameter on Spur Gear Tooth Root and Fillet Stresses." AGMA Paper P229.22, 1981.
18. TAE-HYONG CHONG, A. KUBO. "Simple Stress Formulae for a Thin Rimmed Spur Gear. Part 2: Tooth Fillet and Root Stress Calculation of a Thin Rimmed Internal Spur Gear." ASME Paper No. 84-DET-63, 1984.
19. TAE-HYONG CHONG, A. KUBO. "Simple Stress Formulae for a Thin Rimmed Spur Gear. Part 3: Examination of the Calculation Method and Stress State of Internal Spur Gear." ASME Paper No. 84-DET-64, 1984.
20. TAE-HYONG CHONG, NAOTO KATAYAMA, AIZOH KUBO, HIROSHI YABE. "Tooth Fillet Stresses of Gear with Thin Rim." *Bulletin of the JSME.* Vol. 27, No. 224. February, 1984, 325-332.
21. TAE-HYONG CHONG, NAOTO KATAYAMA, AIZOH KUBO, HIROSHI YABE. "Tooth Fillet Stresses of Gear with

EDITORIAL . . .
(continued from page 6)

Separately, these two show/conferences are important to the industry, stimulating both sales and the exchange of ideas; however, I think a joint effort on the part of AGMA and SME has an even more powerful appeal. Rather than have to support and promote two separate events, they could combine their individual organizational perspectives, strengths and resources to produce an educational event and gear expo of major international importance. A combined effort could also relieve potential exhibitors and attendees with limited budgets of the difficult decision of choosing which event to support. Joint efforts could also, perhaps, produce small technical seminars, conferences and presentations several times a year in different locations to make educational opportunities more accessable to an even greater number of people in the industry.

A third important seed being planted now will directly affect the research and development side of the industry. ASME/Gear Research Institute held two meetings in December of last year to discuss "The Reshaping of U.S. Gear Research." These meetings addressed ways to improve the sharing of gear research among U.S. companies without destroying any competitive advantage to the company developing the research. Also on the agenda was a discussion of various ways to work more closely with university engineering departments to make the most of our applied engineering expertise.

Last, but every bit as exciting, is the Defense Logistics Agency's plans to set up a Gear Manufacturing Research Center whose purpose is to a) conduct and manage gear manufacturing research with the goal of producing aerospace quality (AGMA Class 12 and higher) gears; b) transfer this technology to gear manufacturers as well as producers of equipment for gear manufacturing; and c) integrate the center with an engineering curriculum of a university to train and educate students.

So what difference do all these programs make to you? They're not going to prevent a severe recession, and running your business in a tough economic environment takes all your time and resources. Why should you even care about, much less support, enterprises like these?

Fair questions, but ones that reflect short term thinking. Improving the quality of shows and conferences and of our research efforts pays long-term dividends. It won't, of course, solve current economic problems, and we won't see results on next quarter's bottom line—or even next year's. But these kinds of projects are like planting trees. Carefully nurtured and cared for, they will grow, prosper and provide us with the materials and substance we need to fuel our growth and development in the future.

Michael Goldstein, Editor/Publisher

THE USE OF BOUNDARY. . . *(continued from page 36)*

Thin Rim." *Bulletin of the JSME.* Vol. 27, No. 226. April, 1984, 815-822.

22. N. M. SHOLOMOV. "State of Stress of Central Internal Gear with a Thin Rim." *Russian Engineering Journal.* Vol. 60, No. 4, 1980, 9-12.
23. TERUAKI HIDAKA, TAKESHI ISHIDA, FUMIAKI UCHIDA. "Effects of Rim Thickness and Number of Teeth on Bending Strength of Internal Gear." *Bulletin of the JSME.* Vol. 27, No. 223. January, 1984, 110-116.
24. TERUAKI HIDAKA, TAKESHI ISHIDA, FUMIAKI UCHIDA. "Effects of Addendum Modification Coefficient on Bending Strength of Internal Gear." *Bulletin of the JSME.* Vol. 28, No. 236. February, 1985, 329-336.
25. C. A. BREBBIA. *The Boundary Element Method for Engineers.* Pentech Press, London 1978.
26. P. K. BANNERJEE, R. BUTTERFIELD. *Boundary Element Methods in Engineering Sciences.* McGraw Hill, London. 1981.
27. A. GAKWAYA, A. CARDOU, G. DHATT. "Evaluation of Stresses and Deflection of Spur and Helical Gears by the Boundary Element Method." ASME Paper No. 84-DET-169, 1984.
28. V. RUBENCHIK. "Boundary Integral Equation Method Applied to Gear Strength Rating." ASME Paper No. 82-DET-78, 1982.
29. GORDON H. HOLZE. "Boundary Integral Equation Method Simplifies Elastic Stress Analysis." SAE Paper No. 800431, 1980.
30. J. A. COLLINS. *Failure of Materials in Mechanical Design.* John Wiley and Sons, 1981.
31. SATOSHI ODA, KOUITSU MIYACHIKA, TAKO KOIDE, MASAHITO MIZUNE. "Stress Analysis of Thin Rimmed Spur Gears by Boundary Element Method." *Bulletin of JSME.* Vol. 29, No. 248. Feb., 1986, 593-599.

CALL FOR PAPERS—DEADLINE EXTENSION
INTERNATIONAL CONFERENCE ON GEARING
Zhengzhou, China

Next year, Nov. 5-10, 1988 there will be a three-day conference which will include discussions on theory of tooth form, gear strength and durability, gear materials and heat treatment, dynamics of gear systems, vibration and noise anaylsis, lubrication, non-cylindrical and non-involute gears, power transmissions and standards. The deadline for abstracts (no more than 400 words) of papers has been extended to **May 1, 1988.**

For further information, contact: Inter-Gear '88 Secretariat, Zhengzhou Research Institute of Mechanical Engineering, Zhongyuan Rd., Zhengzhou Henan, China. Tel: 47102, Cable: 3000, Telex 46033 HSTEC CN

Acknowledgement: *Reprinted with permission of the American Gear Manufacturers Association. The opinions, statements and conclusions presented in this article are those of the Authors and in no way represent the position or opinion of the AMERICAN GEAR MANUFACTURERS ASSOCIATION.*

The authors would like to thank the sponsors of the Gear Dynamics and Gear Noise Research Laboratory for their encouragement and financial support which made this study possible.

The editors wish to thank Dennis Gimpert of American Pfauter for his assistance in the technical editing of this article.

BACK TO BASICS...

The Relationship Of Measured Transmission

Robert E. Smith, Consultant
R. E. Smith & Co., Inc.
Rochester, New York

The Gleason Works
Rochester, New York

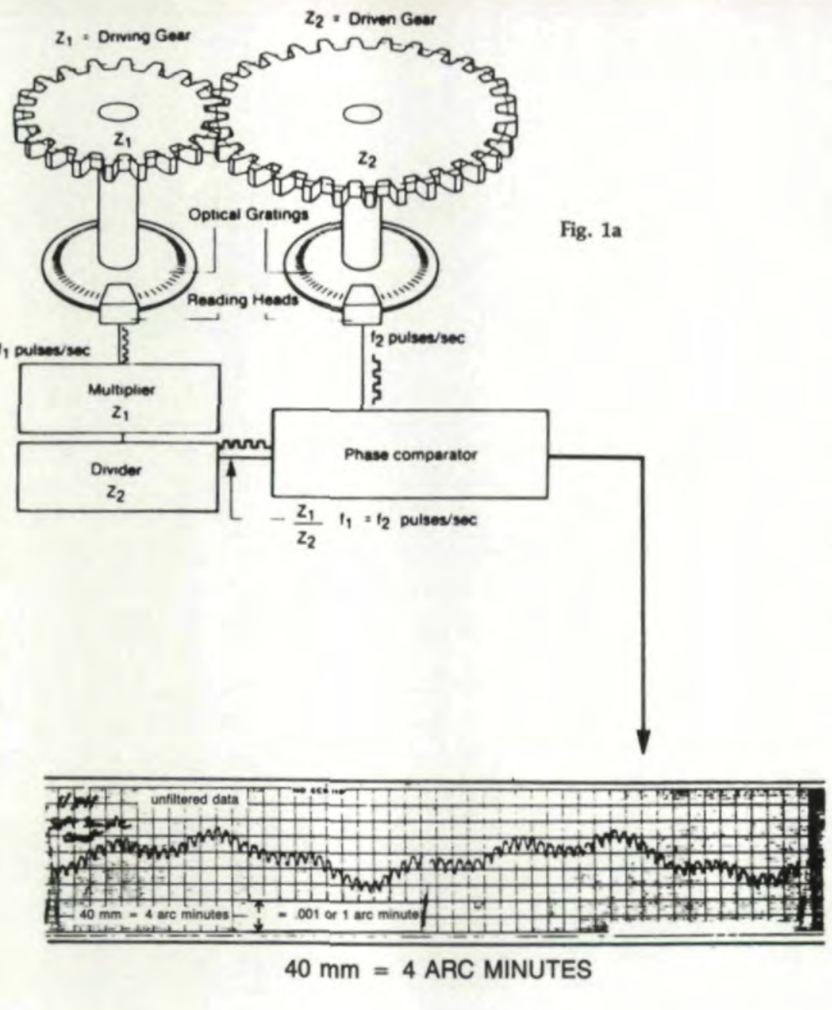

Fig. 1a

Fig. 1b

Abstract

Gear noise is not just a gear problem. It is a system problem and the gears are the exciters of the system. Transmission errors in the gears due to geometric variations are the source of the excitation. This article deals with the instrumented testing of noise in the system and how to successfully relate the results back to the measured transmission errors in the gears. The biggest difficulty in establishing the relationship is how to compare visually displayed sound analysis data to aural judgments of the human rater, and then relate the results back to measured transmission errors of the gears. This is referred to as the "missing link" in the article.

Introduction

Vehicle gear noise testing is a complex and often misunderstood subject. Gear noise is really a system problem.[1] Most gearing used for power transmission is enclosed in a housing and, therefore, little or no audible sound is actually heard from the gear pair.[2] The vibrations created by the gears are amplified by resonances of structural elements. This amplification occurs when the speed of the gear set is such that the meshing frequency or a multiple of it is equal to a natural frequency of the system in which the gears are mounted.

In order to make "quiet" gears, there must be feedback from vehicle testing to gear manufacturing. Unfortunately, this is where a "missing link" usually occurs. Much of the vehicle testing is done in a subjective manner, which is of little help to the gear maker as far as knowing what element of gear quality to improve to reduce noise. If instrumentation is used, such testing is often done by noise and

Gear Noise To Measured Gear Errors

vibration people who know little about gear geometry. Their data may show lots of peak vibrations that bear no relationship to what the human ear is hearing relative to gear quality. Many times the excitation may even be coming from another source, such as a rolling element in a bearing.

Frequency is the key to understanding gear noise. The problem is how to convert aural images to visual ones; in other words, how to find a way to display on a CRT or on paper what the human ear is hearing.

Gears As Exciters of Structures

Most of what we hear as "gear noise" does not come directly from the gear pair at all. The minute vibrations created by the gears as they move through mesh are amplified by resonances in the structural elements of the housing, such as panels, ribs, beams, etc. Gear noise in a vehicle generally occurs at tooth mesh frequency or harmonics of it and occasionally at sidebands of mesh frequency. The gears are the exciter. The structure resonates, amplifies the force and converts it to airborne noise. Transmission error or non-uniform motion of the gears is the mechanism of excitation. Transmission error[3] is the result of small variations from the correct or ideal tooth geometry, as well as runout, and can be measured in the production process by the use of single flank composite testing techniques. In the case of vehicle noise, these variations can be as small as 25 to 150 microinches, depending on the frequency.

Transmission Error Testing

Transmission error testing is done by rolling gears together with backlash and at their proper operating center distance. The input and output angular motion characteristics are measured by an encoder system and electronics as shown in Fig. 1a. The data can be presented in graphic analog form, as shown in Fig. 1b, or can be further processed by Fast Fourier Transform (FFT) techniques to aid in pinpointing the source of excitation. The Fourier technique takes an analog signal and breaks it down into a spectrum of frequencies that relate to the various elements of gear tooth geometry present in the transmission error. (See Fig. 2.) Fig. 3 shows how the geometry of a gear tooth (3a), including flats or waviness, rolls with a master and generates the transmission error curve (3b). This tooth to tooth transmission error curve would be further analyzed by FFT techniques to yield a spectrum as shown in Fig. 3c. The general tooth form or deviations from conjugate tooth shape give rise to the integer harmonics in the spectrum; waviness or flats relate to the "ghost" harmonics; and the long term errors (runout) cause the sidebands of tooth mesh frequency. See References 1

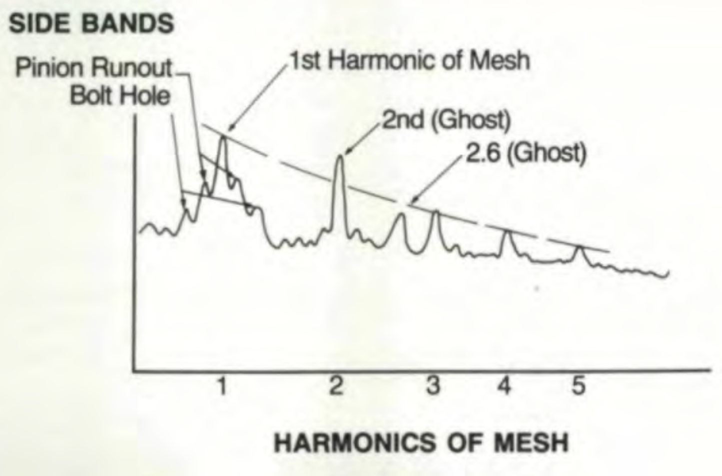

Fig. 2

AUTHOR:

MR. ROBERT E. SMITH *has over thirty years experience in the gear industry. He is currently president of R.E. Smith and Company, a consulting firm in Rochester, New York. He received his training from Rochester Institute of Technology. While employed by The Gleason Works, his engineering assignments included gear methods, manufacturing, research and gear quality. These assignments involved the use and application of instrumentation for the study of noise, vibration and structural dynamics. From these assignments, he expanded his ideas relating to gear metrology. Currently, Mr. Smith is chairman of the Measuring Methods and Practices and Master Gear Subcommittee, AGMA, and is also a member of the Rochester Industrial Engineering Society and the Society of Experimental Stress Analysis.*

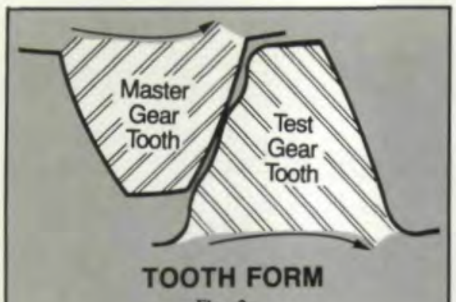

Fig. 3a

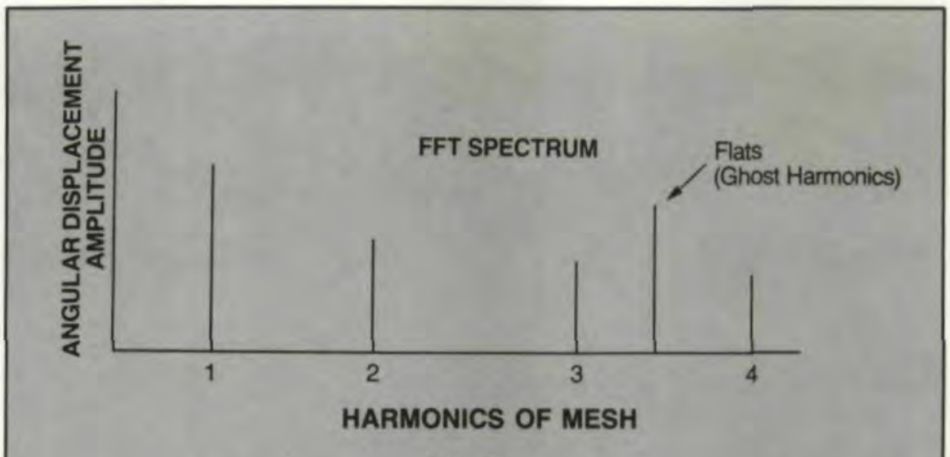

Fig. 3c

and 3 for further discussion of this subject.

The Missing Link

After the gears have been measured by single flank composite testing and all of the possible excitation sources have been identified, it is necessary to put the gears in the final application and measure the results. This is where the "missing link" usually is obvious. The missing link is "frequency discrimination". (See Fig. 4.) Many facilities at this point only use subjective rating techniques. A human rater judges the level of "gear" noise on a scale of one to ten. Ten is inaudible; five is borderline acceptable, and four is reject. Unfortunately, the rater may be rating on first harmonic of mesh in one test and second harmonic or a ghost harmonic in another test. He or she may even by listening to noise as excited by bearings rather than gears, even though the noise sounds like the gears.

Fig. 4

The problem is that the vehicle is generating noise at many frequencies due to road and tire conditions, wind, engine, transmission components, final drive gears, etc. This masking noise or ambient noise level (Fig. 5) is several dB higher than the gear noise the human ear is sorting out and finding objectionable.[2] Even if instrumentation is used to evaluate the vehicle test, the displays or hard copy of data may show many peaks or frequencies unrelated to what the subjective rater is hearing. The challenge is to be able to sort out the important frequencies and relate visual data to aural observations.

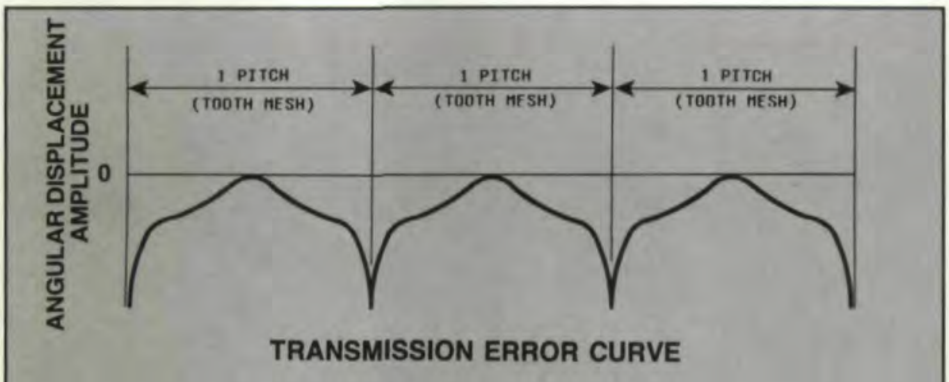

Fig. 3b

Types of Vehicle Sound Testing

Two basic types of vehicle noise testing will be discussed here. Type I, frequency discrimination, involves identifying the problem — the "missing link" referred to above. Type II involves comparing the relative noise levels of various gear boxes as traditionally done with tracking filters.

Type I Noise Testing.

This is the most important "first step" to vehicle noise testing. As mentioned above, frequency is the key to understanding gear noise. The purpose of Type I noise testing is to properly use frequency discrimination to relate what the human ear is hearing to what the eye sees in graphic data related to gear transmis-

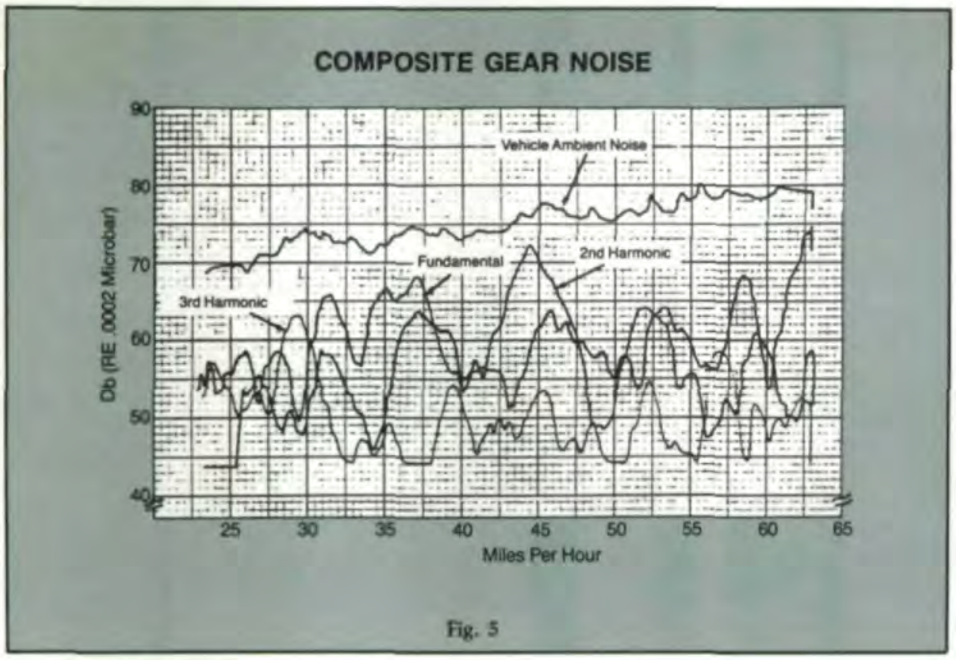

Fig. 5

sion errors. The necessary test equipment is pictured in Fig. 6.

Test Equipment:

1. Real time spectrum analyzer (RTA) with bubble memory.
2. Sound pressure level meter.
3. 12 VDC to 110 VAC Inverter compatible with microprocessor equipment.
4. Tachometer pulse generator and readout attached to drive shaft. (optional)
5. Tape recorder. (optional)
6. Digital plotter for hard copy of RTA data. (optional)

Test Procedure:

1. Calculate and plot ahead of time the drive shaft RPM vs. gear mesh frequencies at all vehicle speeds. This information can be used, along with the tachometer readout in the vehicle to identify mesh frequencies at any time during the test. (See Fig. 7a.)
2. Install the equipment listed above, except for the digital plotter, in the vehicle under test. Be sure to choose a gear box that is a definite reject or noisy example. It may be necessary to run several tests to find the optimum location for the microphone.
3. Make a test drive with the vehicle piloted by a qualified subjective rater and an instrument technician to operate the RTA and adjust it to optimize the display to relate to the subjective rater.
4. Set the analyzer to operate in Mode I to detect the peak noise frequencies at different vehicle speeds or Mode II to detect the resonant frequencies of the structure.
5. Mode I setup—Peak noise frequencies

Sound Pressure Level Meter	A Weighted
RTA Frequency Range	0 to 2000 Hz (1)
Voltage Scale Y Axis (log)	0 to 10 volts RMS
Input	A Weighted (2)
RMS exponential averaging	(3 or 4 averages)

Cursor identifying "peak" amplitude

NOTES:

(a) Frequency range will vary according to application.

(b) This results in an unconventional "double A" weighting. This is in order to enhance data in relation to what the ear is hearing and could be done by the use of other high and low pass filters.

6. Operate the vehicle at a speed and condition that allows the driver to hear gear noise. Then change vehicle speed and load conditions up and down through this noise period. The noise should change in amplitude or come and go. While the driver is doing this, the instrumentation operator can observe which peak in the frequency spectrum is varying in relation to what the driver is hearing. The cursor on the screen will indicate the frequency of interest. The frequency and RPM should be written in a test log. Tape recordings can be made, and the data on the RTA screen can be stored in bubble memory for plotting at a later time. The vehicle can then be driven at any other speed of interest and the test procedure repeated.
7. If desired, run the test in a slightly different manner. The vehicle can be accelerated or decelerated throughout a broad speed range. The RTA screen is observed throughout the test. The cursor will automatically shift to the highest noise level at any given speed. The frequency of the cursor location would be noted on the "fly" and may peak at one, two or several frequencies throughout the speed range.
8. Mode II setup — Structural resonances

   The setup for Mode II operation is the same as for Mode I, except for the cursor operation. The cursor should now be set for "peak hold" mode. The test would be run as described in Step 7. At the end of an acceleration or deceleration run, the display is held (pause) and stored in bubble memory or analyzed for peak frequencies. The

Fig. 6

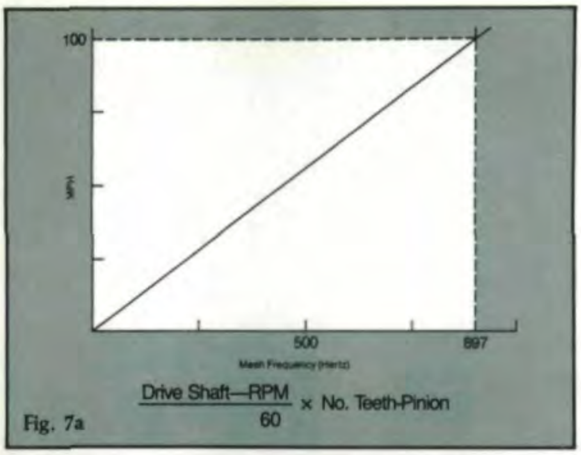

Fig. 7a

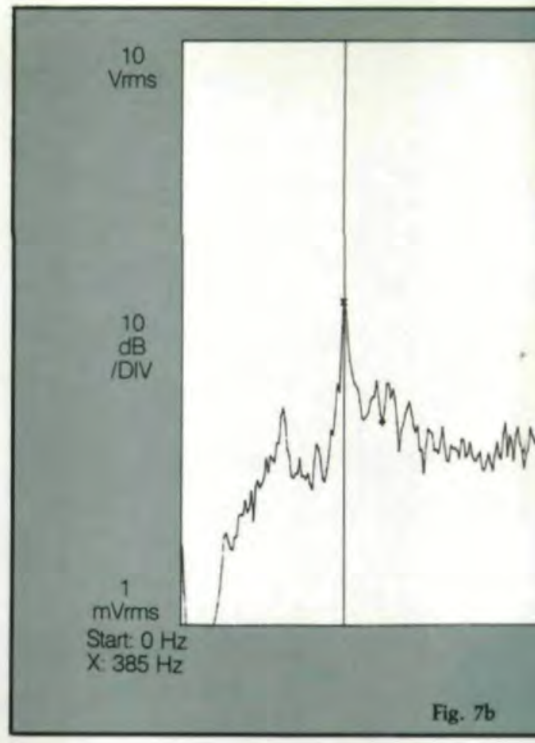

Fig. 7b

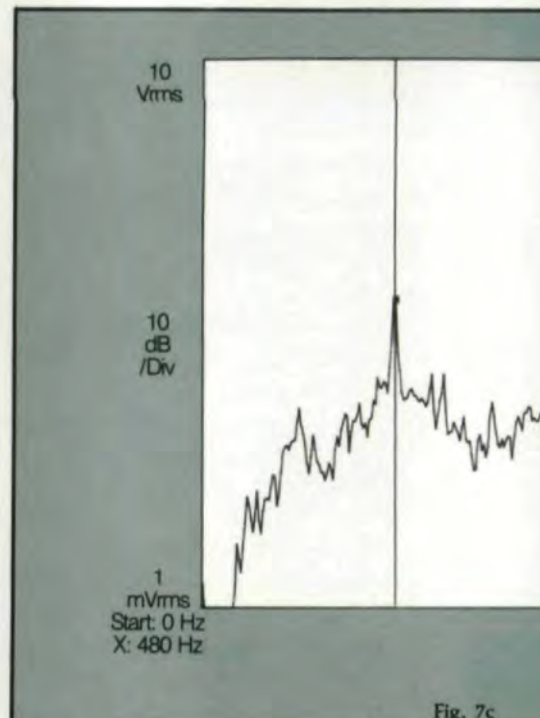

Fig. 7c

peaks in this display represent the structural resonant frequencies. These frequencies could be excited at any vehicle speed by the appropriate mesh frequency or harmonics that happen to coincide.

9. Compare the frequencies of gear mesh and the harmonics and sidebands determined from this test with the gear mesh and harmonic data generated in the single flank transmission error tests of the same gear sets. In

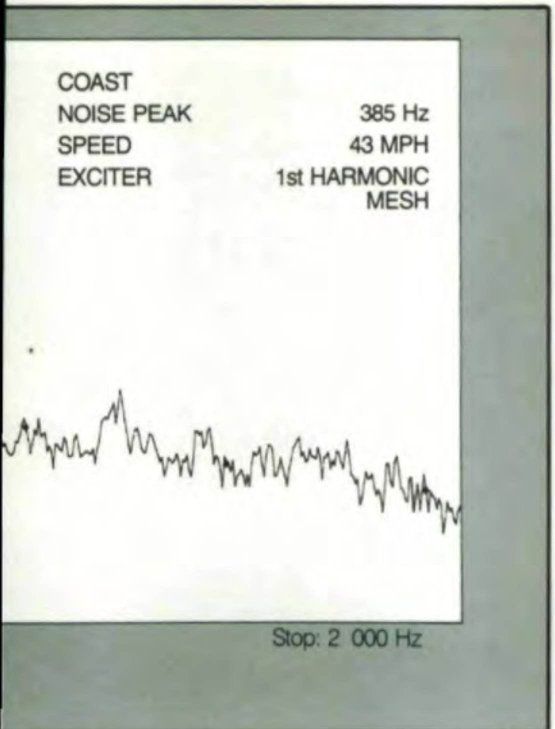

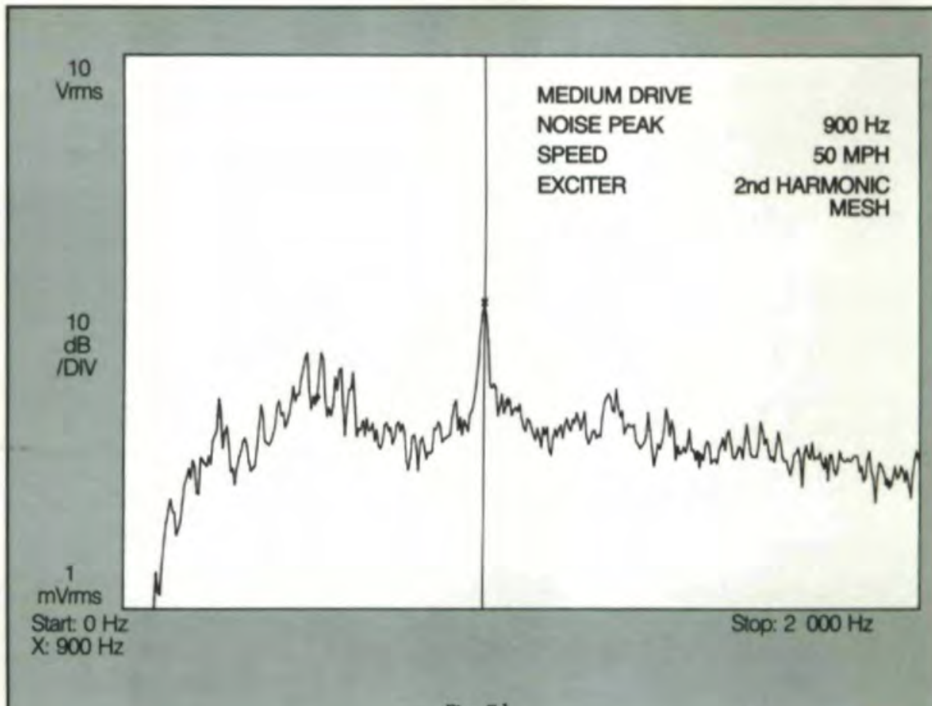

Fig. 7d

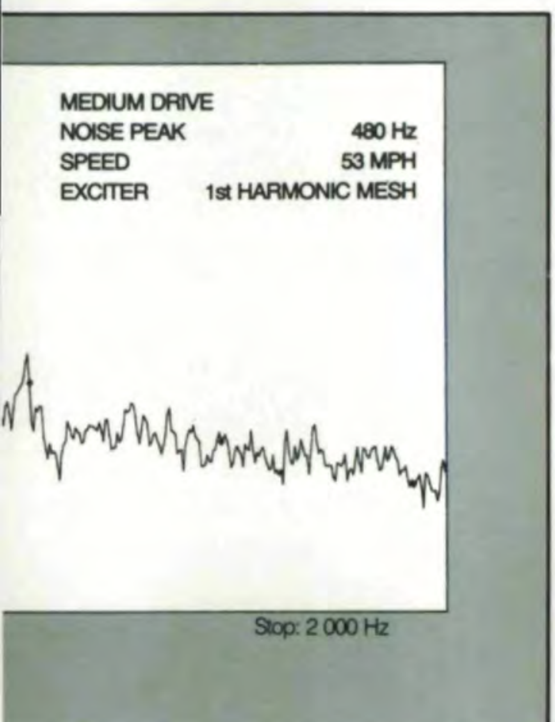

this way, characteristics of the gear tooth geometry can be related to the causes of gear noise in the vehicle. (See Figs. 7b, 7c, 7d.)

Type II Noise Testing.

Comparing the relative level of noise from one gear box to another has been done for many years by a method as described in Reference 2. This involves the use of tracking filters. These are narrow band pass filters of 5 or 10 Hz bandwidth that are tuned by pulses from a tach generator on the drive shaft, such that the center frequency is always at mesh frequency or some harmonic of it. As the vehicle varies speed, the filter is always tuned to a particular order of rotation of the drive shaft. A plot of the output of the filter will show any peak noises associated with the gear mesh at that particular order of rotation. The vehicle can be driven at various rates of acceleration and deceleration and a complete history recorded for analysis. The results are quite accurate and repeatable, so it is useful for the comparison of two or several gear boxes. Fig. 8 shows the

Vehicle Recording Unit

FLEXA-TROL™

High Intensity, Multi-Frequency Scanners

REDUCE HEAT TREATING COSTS up to 40%

A recent TOCCO development, High Intensity Induction Hardening (HIIH)™, reduces heat treating costs substantially, in a variety of applications. HIIH has been used successfully with applications on automotive and off-highway engine and drive train components, as well as specialized gear applications. The HIIH scanning process, with present technology, can be adapted to parts up to 15″ diameter and lengths to 120″.

Parts that previously were flame hardened in a batch process, can now be induction hardened, in-line, with greater flexibility, more precision, individual quality monitoring, and at lower cost.

High Intensity Induction Hardening is indeed, a process of "The Future".

HIGH INTENSITY HARDENING PATTERNS

Cross section of camshaft lobe demonstrates uniformity of hardening. Multi-frequency, high intensity hardening of gears produces a high hardness characteristic for improved surface contact fatigue life. High residual compressive stress in the root area is also achieved for improved tooth strength.

For the latest state-of-the-art heat treating technology, contact your TOCCO representative, or call: TOCCO, Inc., 30100 Stephenson Highway, Madison Hts., MI, 48071. Phone: 313-399-8601 or 1-800-468-4932 (outside Michigan).

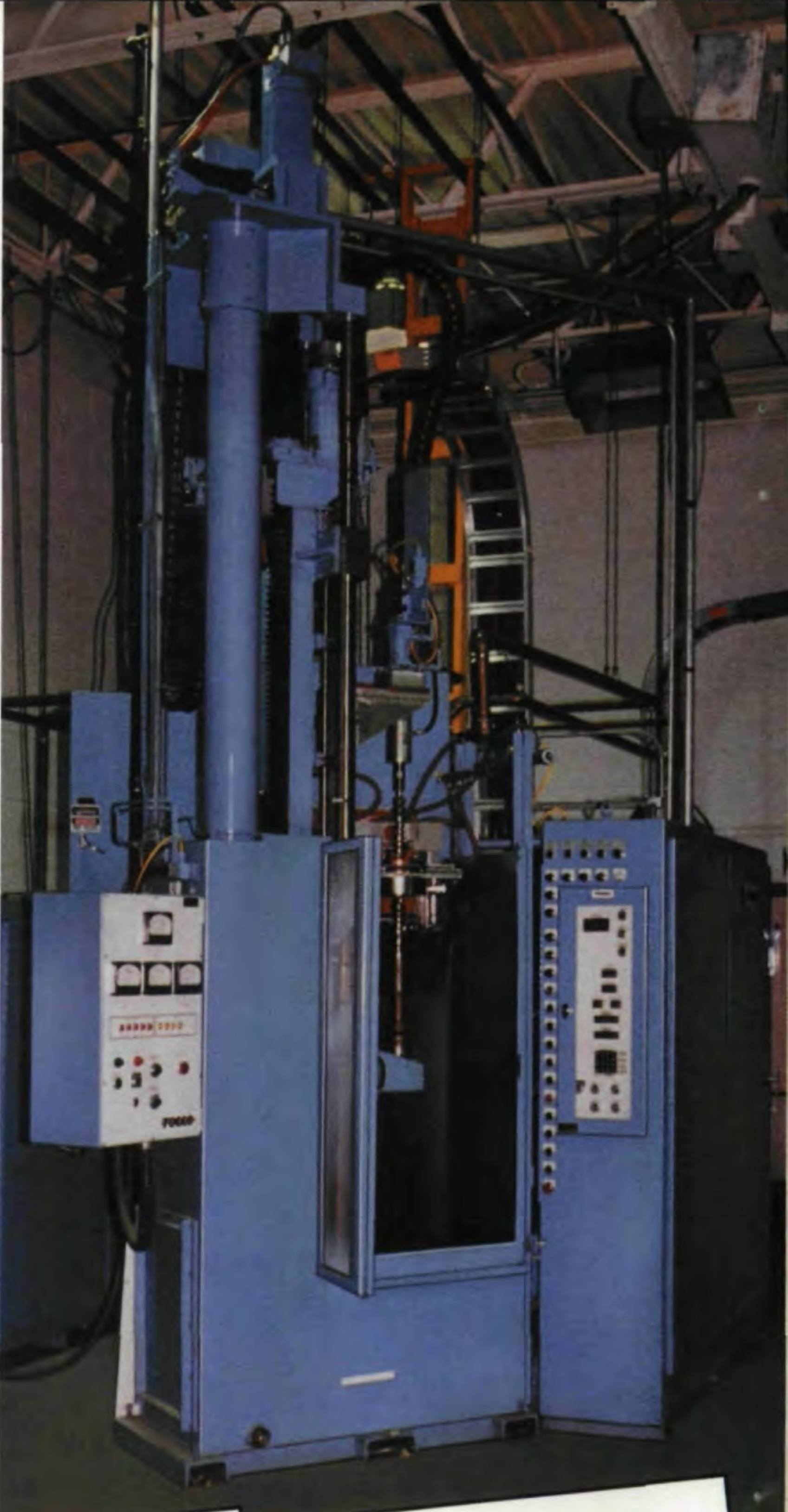

NEW . . . TDS
TOCCO System Diagnostics are offered to document Induction System performance during dynamic, fault or standby conditions. This advanced TDS monitors digital and analog signals while recording, printing or modem transferring data to designated locations for system performance evaluation or trouble-shooting. Ask your TOCCO sales engineer for further details.

TOCCO®

A unit of Park Ohio Industries, Inc.

CIRCLE A-12 ON READER REPLY CARD

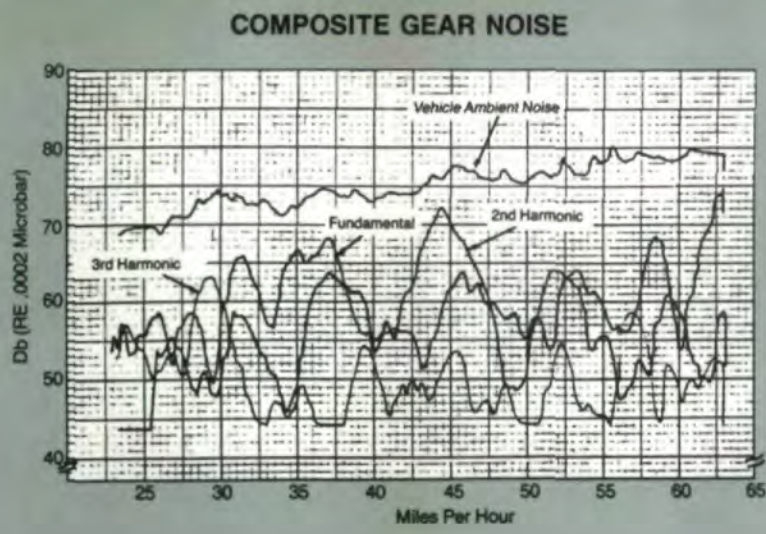

Fig. 8

test setup and results from such a system. There is a trend today to try to do this kind of analysis with digital Fast Fourier Transform (FFT) techniques, rather than with analog tracking filters. However, it is questionable whether the digital techniques are fast enough to detect the peak noise periods with sufficient accuracy when the vehicle is constantly changing speed. The FFT techniques are acceptable in Type I testing because only the frequency, not the relative amplitudes, is of interest. In Type II testing, one is trying to catch the absolute maximum amplitude for each set of gears being tested. There are times when the noise is heard only as the vehicle is changing speed or load conditions.

Case History

NOTE: Because permission was given by a European auto maker to use actual test results for this article, it was decided to present the data in metric units, kilometers per hour (KPH), rather than convert to MPH.[4]

During the process of installing a single flank transmission error tester at an automotive plant, a study was run to correlate transmission error with vehicle gear noise. Single flank data was analyzed by FFT techniques to quantify excitation related to first, second and other harmonics of mesh for several gear sets. The same gear sets were built in a test vehicle and rated subjectively for noise level during road tests. The vehicle was also instrumented and noise tested on a dynomometer test stand using FFT analytical techniques.

The data from the single flank test, subjective road test and instrumented dynomometer test was then compared for correlation. The results did not look good for several reasons.

In a subjective test, the driver rates noise heard at any speed on a scale from one to ten. He or she may rate one gear set for noise heard at 80 KPH caused by second harmonic of mesh and another set for noise heard at 160 KPH caused by first harmonic of mesh. The noise sounds the same, and the rater does not realize the excitation is coming from different sources. In fact, at some other speed a similar noise was being caused by excitation from bearings used to mount the pinion.

In the instrumented dynomometer test, FFT analyses were run at given fixed speeds. These resulted in spectral data showing peaks at many frequencies. The problem is to determine the one to which the driver is responding. When looking at first harmonic data from single flank and dynomometer tests vs. subjective ratings, the correlation was poor. The same was true when comparing only the second harmonic data. The assumption was that all gear noise was coming from the same source of excitation.

A new test was then started by using the techniques described above for Type I Noise Testing. It was not feasible to run the RTA in the vehicle at that time, so a decision was made to tape record the road test data and analyze it later in the laboratory. This was done for several road tests with different gear sets. Subsequent analysis showed that the noise heard at 80 KPH was excited by second harmonic of mesh, at 160 KPH by first harmonic of mesh, and at 40 KPH at fourth harmonic of mesh. In all cases the frequency of noise was approximately 930 Hz. Now when the single flank data of first harmonic transmission error was compared to subjective ratings at 160 KPH, and the single flank second harmonic was compared to subjective ratings at 80 KPH independently a good correlation was shown.

(continued on page 47)

Gear Sound
Analysis Console

CLASSIFIED

Rates: Classified Display—per inch (minimum 3") **1X**-$120, **3X**-$110, **6X**-$100. Type will be set to advertiser's layout or *Gear Technology* will set type at no extra charge. **Word Count:** 35 characters per line, 7 lines per inch.

Payment: Full payment must accompany classified ads. Mail copy to *Gear Technology*, P.O. Box 1426, Elk Grove Village, IL 60007. **Agency Commission:** No agency commision on classifieds.

Materials Deadline: Ads must be received by the 25th of the month, two months prior to publication. **Acceptance:** Publisher reserves the right to accept or reject classified advertisements at his discretion.

COMPUTER AIDS

HELP WANTED

BUSINESS OPPORTUNITIES

RELATIONSHIP OF MEASURED GEAR NOISE . . .

(continued from page 45)

With this knowledge, another program was started with a greater number of axles and yielded excellent results, even when comparing single flank transmission errors against subjective car ratings. (See Fig. 9.) From this data it was possible to establish an acceptable range of single flank transmission errors for first and second harmonics of mesh.

Conclusion

Many different types of instrumentation are available for the sound testing of gear noise. However, the procedure used with the instruments is the key to successful application. Relating the frequency of the noise aurally and visually in the data is the most important step in the analysis.

It is possible to apply the above techniques and sort out the facts from mystery. Once this is done, a correlation between noise and transmission error can be established and limits can set on the process for quality control.

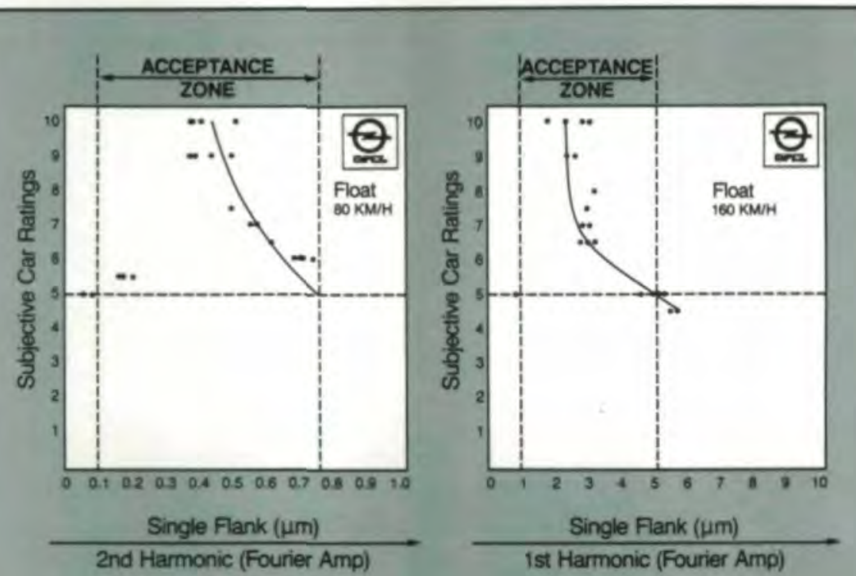

Fig. 9

References:

1. SMITH, R.E. "Identification of Gear Noise With Single Flank Composite Measurement," AGMA Fall Technical Meeting, San Francisco, CA, October 14-16, 1985.
2. PITTS, L.S. "Bevel and Hypoid Gear Noise Reduction," SAE Paper No. 720734.
3. SMITH, R.E. "What Single Flank Measurement Can Do For You," AGMA Fall Technical Meeting, Washington, D.C., October 15-17, 1984.
4. VONDERSCHMIDT. Data from testing done at Adam Opel AG., Ruesselsheim, West Germany.

Acknowledgement: *The author wishes to thank Adam Opel AG., Ruesselsheim, West Germany, and Dr. Vonderschmidt for the use of their test data.*

DESCRIBING NONSTANDARD GEARS . . .
(continued from page 27)

Appendix C — Survey Results

Five gear designers in the US and two in Europe were asked to determine the x factor for the following gear set, which is used in a high speed, high shock application:

Center Distance	6.000/6.005"	
Spur Gears		
Normal Diametral Pitch	5	
Hob Profile Angle, Normal	20°	
Base Pitch	.5904263"	
Hob Addendum	.280"	
Hob Tooth Thickness	.314"	
	PINION	GEAR
Number of Teeth	23	35
Base Tangent Length	1.590/1.588"	2.257/2.254"
Tooth Thickness at Std. Dia.	.369/.367"	.413/.410"
Outside Diameter	5.130/5.125"	7.655/7.650"

The following data was calculated, but not provided:

Minimum Backlash	.0108"	
X (OD Method)	.3250	.6375
Backlash Allowance	−.0054"	−.0056"
X (TT Method)	.3619	.6759

SURVEY RESPONSES

	X_1	X_2	SUM
A	.3250	.6375	.9625
B	.3619	.6759	1.0375
C	.3688	.6676	1.0364
D	.3804	.6829	1.0633
E	.4000	.7169	1.1169
F	.4994	.8016	1.3010
Average	.3892	.6971	1.0863
Range	+28/−16.5%	+14.9/−8.6%	+19.7/−11.4%

References

1. *Maag Gear Book.* Maag Gear Wheel Company, Ltd. Zurich, Switzerland. 1963.
2. *Gear Cutting Tools. Manual for Design and Manufacturing.* Third Edition. Verzahntechnik Lorenz GMBH. Ettlingen, West Germany. 1980.
3. Isthmian Canal Commission. *Miter Gate Moving Machine — Crank Gear, Pinion and Tooth Profile.* Dwg. No. 6219. Culebra, Canal Zone, Panama. 1911.
4. GROSSER, C.E. "Involute Gear Geometry." ASME Paper No. 48-A-73. American Sociey of Mechanical Engineers. New York, NY. 1948.
5. *Farrel Gear Manual for Herringbone, Helical and Spur Gears.* Bulletin 610A. Farrel-Birmingham Company, Inc. Rochester, NY. 1961.
6. COOPER, D.W. *Digital Computers in Engineering Analysis.* Penton Publishing Co. Cleveland, OH. 1962. pp. 16-17.
7. ERRICHELLO, R.L. "Calc Program Finds Inverse Involute." *Machine Design,* March 8, 1979.
8. LASKIN, I. *AGMA News Digest.* Vol. 43, No. 5. Nov., 1984.
9. *Modern Methods of Gear Manufacture.* National Broach & Machine Division/Lear Siegler. Detroit, MI 1972.

Acknowledgment: *Reprinted with permission of the American Gear Manufacturers Association.*

The opinions, statements and conclusions presented in this article are those of the author and in no way represent the position or opinion of the AMERICAN GEAR MANUFACTURERS ASSOCIATION.

Special thanks to John Leming of Arrow Gear, Kevin Acheson of The Gear Works — Seattle, Inc., Dan Thurman of Caterpillar Tractor, Bob Errichello of Geartech, Len Haas of Speco Div., Kelsey Hayes and Irv Laskin for their help in preparing this article.

KHV PLANETARY GEARING . . .
(continued from page 32)

References

1. MOROZUMI, MUNEHARU. "The Efficiency and the Design of Modified Internal Gearing," *Mechanical Researches,* No. 5, pp. 720-726, 1970 (Japanese).
2. BOLOTOVSKAYA, T.P. *Calculation for Modified Gears by Block Diagrams,* UFA, 1958 (Russian).
3. YU, DAVID, "Discussion on the Methods for Calculating Geometrical Dimension of Internal Gearing," *Mining Machine,* No. 4, pp. 72-78, 1980 (Chinese).
4. BOLOTOVSKAYA, T.P. *Geometrical Calculation Handbook for Involute Gear and Worm Transmissions,* Machine Building Publishing House, 1963, (Russian).
5. GAVLILENKO, V.A. *Gear Transmission of Machine Building* Machine Building Publishing House, 1962 (Russian).
6. KUDLYAVTZEV, V.H. *Planetary Transmission,* Machine Building Publishing House, 1966 (Russian).
7. YU, DAVID. "Problems Arising in the Calculation of Gearing Efficiency," *Liaoning Machine,* No. 2, pp. 33-42, 1980 (Chinese).
8. MOROZUMI, MUNEHARU, "The Efficiency of Hypocycloid Gear Reducer with Minimum Tooth Difference," *Journal of the Faculty of Engineering,* Shinshu University, Japan, No. 31, pp. 119-128, 1971.
9. YASTLEBOV, B.M. "On Contact Ratio of Internal Meshing With Small Tooth Difference", *Science Bulletin of Machine Building,* No. 8, pp. 23-30, 1965 (Russian).
10. MOKHTAR, S.B. and C.M. SHETTY, *Nonlinear Programming.* John Wiley & Sons, Inc., 1979.

Acknowledgement: *Reprinted from International Symposium on Gearing and Power Transmissions, Tokyo, Japan, 1981.*

When it comes to gear machining needs, Mitsubishi cuts the leading edge.

GA15CNC

GA25CNC

GA63CNC

SA25CNC

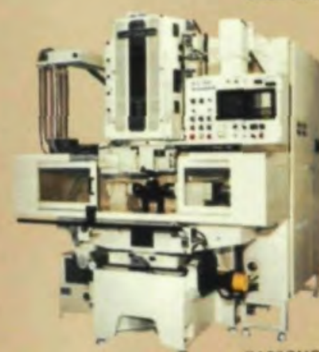

FA30CNC

Gear Cutting Tools

Mitsubishi mechanical and electronic technologies come together today in a full lineup of the most advanced gear cutting machines on the market. Whether your requirements call for hobbing, gear shaping or gear shaving, including flexible gear manufacturing systems, Mitsubishi offers the ideal solution for any need. All machines are unsurpassed in flexibility, speed, accuracy and rigidity — resulting in new standards of productivity. For full information on the entire lineup, along with available tools, contact us today.

SPECIFICATIONS

Model		Max. Workpiece Dia. (in)	Max. Workpiece Pitch (D.P.)	Main Motor (HP)	Machine Weight (Lbs)
Gear Hobbers	GA15CNC	5.9/7.9	6.35	10	8,800
	GA25CNC	9.8	4	10	17,600
	GA40CNC	15.7	4	10	18,700
	GA63CNC	24.8	1.8	20	24,200
Gear Shapers	SA25CNC	9.8	4	7.5	11,000
	SA40CNC	15.7	4	10	15,600
	SA63CNC	25.6	3.2	24.7	21,100
Gear Shaver	FA30CNC	12.2	3.2	7.5	11,500

MITSUBISHI
HEAVY INDUSTRIES, LTD.
5-1, Marunouchi 2-chome, Chiyoda-ku, Tokyo, Japan
Cable Address: HISHIJU TOKYO

Mitsubishi Heavy Industries America, Inc.
873 Supreme Drive, Bensenville, IL 60106 Phone: (312) 860-4220

Mitsubishi International Corporation
873 Supreme Drive, Bensenville, IL 60106 Phone: (312) 860-4222